$b \to s\bar{l}l$ in the minimal supergravity model

Toru Goto,[1] Yasuhiro Okada,[2] Yasuhiro Shimizu,[1,2] and Minoru Tanaka[3]
[1]*Department of Physics, Tohoku University, Sendai 980-77 Japan*
[2]*Theory Group, KEK, Tsukuba, Ibaraki, 305 Japan*
[3]*Department of Physics, Osaka University, Toyonaka, Osaka, 560 Japan*
(Received 30 September 1996)

The $b \to s l^+ l^-$ process is studied in the minimal supergravity model in detail. Taking into account the long-distance contributions from the $c\bar{c}$ resonances, we calculate the branching ratio and the lepton forward-backward asymmetry in this model. We find that there is a strong correlation between the branching ratios of $b \to s\gamma$ and $b \to s l^+ l^-$ processes and that the interference effect can change the $b \to s l^+ l^-$ branching ratio in the off-resonance regions by up to $\pm 15\%$ depending on the relative phase between the long- and short-distance contributions. Using various phenomenological constraints including the branching ratio of $b \to s\gamma$, we show that there are regions in the parameter space where the branching ratio of $b \to s l^+ l^-$ is enhanced by about 50% compared to the standard model (SM). We also show that the branching ratio of $b \to s\nu\bar{\nu}$ is reduced at most by 10% from the SM prediction. [S0556-2821(97)04707-3]

PACS number(s): 13.20.He, 12.60.Jv, 14.65.Fy

I. INTRODUCTION

Although the standard model (SM) of the elementary particle physics is successful in explaining almost all experimental results, it is possible that physics beyond the SM exists just above the presently available energy scale. Since new physics may affect various processes at low energy such as the flavor-changing neutral current (FCNC) processes of K mesons and B mesons, new physics searches in these processes are as important as direct particle searches at collider experiments. A prime example is the $b \to s\gamma$ process. Experimentally the inclusive branching ratio is determined as $B(b \to s\gamma) = (2.32 \pm 0.57 \pm 0.35) \times 10^{-4}$ at the CLEO experiment [1]. It is known that this process puts very strong constraints on various new physics beyond the SM, for example, two-Higgs-doublet model and supersymmetric (SUSY) extension of the SM. Along with the $b \to s\gamma$ process, another important rare b decay process is the $b \to s\bar{l}l$ decay. Although only upper bounds on branching ratios are given by experiments for various exclusive modes [2], this process is expected to be observed in the near future at B factories as well as at hadron machines.

In this paper we investigate the $b \to s\bar{l}l$ decay in the minimal supersymmetric standard model (MSSM), especially in the minimal supergravity (SUGRA) model. The MSSM is now considered to be the most promising candidate beyond the SM. In the MSSM, SUSY partners such as squarks, sleptons, Higgsinos, and gauginos can contribute to FCNC processes through loop diagrams. In order to evaluate their contributions quantitatively it is necessary to specify how soft SUSY-breaking terms are generated. In particular, the soft SUSY-breaking terms in the squark sector become new sources of flavor mixing, and the K^0-$\bar{K}^0$ mixing becomes too large if the squark mixing is of order 1 and masses of SUSY partners are in the below-TeV region [3]. In the minimal SUGRA model it is assumed that the soft SUSY-breaking terms are universal at the Planck or grand-unified theory (GUT) scale. Flavor mixing at the electroweak scale can be determined by solving the relevant renormalization-group equations (RGE's) from the Planck to the low-energy scale. It is shown that the constraint from the K^0-$\bar{K}^0$ mixing is easily satisfied in this framework since masses of the first two-generation squarks with the same quantum numbers remain highly degenerate at the low energy [3]. The FCNC processes involving the third-generation quarks and squarks can receive sizable SUSY contributions due to the large top Yukawa coupling constant. In particular the $b \to s\gamma$ process has been intensively studied both in low-energy SUSY standard models and in the minimal SUGRA model [4–6]. It was observed that the SUSY loop effects can interfere with the SM amplitude constructively or destructively depending on the parameters on the model whereas the charged Higgs contribution is always constructive. For the minimal SUGRA model the B^0-$\bar{B}^0$ mixing and CP-violating parameter in the K^0-$\bar{K}^0$ mixing, ϵ_K, has also been investigated in [7]. In this paper we consider the $b \to s\bar{l}l$ process in addition to the $b \to s\gamma$ process to see possible implication on the model by future experiments. We observe that the predicted branching ratio of the $b \to s\gamma$ process and that of the $b \to s l^+ l^-$ process are strongly correlated and thus their measurements are useful to distinguish the SUGRA model from other extensions of the SM.

The $b \to s l^+ l^-$ process in the SUGRA model was analyzed by Bertolini *et al.* in [4]. Recently this process was reconsidered taking account of the measured branching ratio of $b \to s\gamma$ and the top-quark mass in the context of the low-energy SUSY models as well as the minimal SUGRA model [8,9]. In [8] it was noted that the $b \to s l^+ l^-$ process is able to resolve twofold ambiguity which cannot be distinguished from the branching ratio of $b \to s\gamma$. In [9] a more detailed analysis has been done in the minimal SUGRA model. Compared to them, our calculation is improved in several points such as (1) numerically solving RGE's with whole Yukawa matrices and soft SUSY-breaking parameters with the flavor mixing, (2) taking account of one-loop corrections in the Higgs effective potential [10] in order to determine the

proper vacuum expectation value through the radiative electroweak symmetry-breaking scenario [11], and (3) including the interference effect with the long-distance contribution in calculating the lepton invariant mass spectrum of the $b\to sl^+l^-$ branching ratio. It turns out that the third effect can change the branching ratio in the off-resonance region by $\sim\pm 15\%$ depending on the relative phase between the long- and short-distance contributions. Taking account of various phenomenological constraints including the branching ratio of $b\to s\gamma$, we show that there are regions in the parameter space where the branching ratio of $b\to sl^+l^-$ is enhanced by about 50% compared to the SM. We also calculate the branching ratio of the $b\to s\nu\bar{\nu}$ process in the minimal SUGRA model and show that the branching ratio is reduced at most by 10% from the SM value.

This paper is organized as follows. In Sec. II, we introduce the minimal SUGRA model and explain new sources of flavor changing in this model. In Sec. III, formulas for $b\to sl^+l^-$ decay are given including SUSY contributions. In Sec. IV, we present numerical results of our analysis. In Sec. V, $b\to s\nu\bar{\nu}$ decay is discussed. Section VI gives conclusions and discussions. Various formulas are summarized in the Appendices.

II. MINIMAL SUGRA MODEL

The MSSM Lagrangian is specified by the superpotential and the soft SUSY-breaking terms. The superpotential of the MSSM is given by

$$W_F=\epsilon_{\alpha\beta}[f_{Uij}Q_i^\alpha H_2^\beta U_j+f_{Dij}H_1^\alpha Q_i^\beta D_j+f_{Eij}H_1^\alpha L_i^\beta E_j-\mu H_1^\alpha H_2^\beta], \tag{2.1}$$

where the chiral superfields Q, U, D, L, E, H_1, and H_2 transform under $\mathrm{SU}(3)_C\times\mathrm{SU}(2)_L\times\mathrm{U}(1)_Y$ as the representations

$$Q_i^\alpha=\left(3,2,\frac{1}{6}\right),\quad U_i=\left(\overline{3},1,-\frac{2}{3}\right),\quad D_i=\left(\overline{3},1,\frac{1}{3}\right),$$

$$L_i^\alpha=\left(1,2,-\frac{1}{2}\right),\quad E_i=(1,1,1), \tag{2.2}$$

$$H_1^\alpha=\left(1,2,-\frac{1}{2}\right),\quad H_2^\alpha=\left(1,2,\frac{1}{2}\right).$$

The suffixes $\alpha,\beta=1,2$ are SU(2) indices and $i,j=1,2,3$ are generation indices. $\epsilon_{\alpha\beta}$ is the antisymmetric tensor with $\epsilon_{12}=1$. A general form of the soft SUSY-breaking terms is given by

$$\begin{aligned}-\mathcal{L}_{\mathrm{soft}}=&(m_Q^2)_{ij}\tilde{q}_{Li}^{\dagger}\tilde{q}_{Lj}+(m_U^2)_{ij}\tilde{u}_{Ri}^{*}\tilde{u}_{Rj}+(m_D^2)_{ij}\tilde{d}_{Ri}^{*}\tilde{d}_{Rj}+(m_L^2)_{ij}\tilde{l}_{Li}^{\dagger}\tilde{l}_{Lj}+(m_E^2)_{ij}\tilde{e}_{Ri}^{*}\tilde{e}_{Rj}+\Delta_1^2h_1^{\dagger}h_1+\Delta_2^2h_2^{\dagger}h_2\\&+\epsilon_{\alpha\beta}(B\mu h_1^\alpha h_2^\beta+\mathrm{H.c.})+\epsilon_{\alpha\beta}(A_{Uij}\tilde{q}_{Li}^\alpha h_2^\beta\tilde{u}_{Rj}^{*}+A_{Dij}h_1^\alpha\tilde{q}_{Li}^\beta\tilde{d}_{Rj}^{*}+A_{Eij}h_1^\alpha\tilde{l}_{Li}^\beta\tilde{e}_{Rj}^{*}+\mathrm{H.c.})\\&+\left(\frac{1}{2}m_{\tilde{B}}\tilde{B}\tilde{B}+\frac{1}{2}m_{\tilde{W}}\tilde{W}\tilde{W}+\frac{1}{2}m_{\tilde{G}}\tilde{G}\tilde{G}+\mathrm{H.c.}\right),\end{aligned} \tag{2.3}$$

where $\tilde{q}_{Li}$, $\tilde{u}_{Ri}^{*}$, $\tilde{d}_{Ri}^{*}$, $\tilde{l}_{Li}$, $\tilde{e}_{Ri}^{*}$, and h_1, and h_2 are scalar components of chiral superfields Q_i, U_i, D_i, L_i, E_i, H_1, and H_2 respectively, and $\tilde{B}$, $\tilde{W}$, and $\tilde{G}$ are $\mathrm{U}(1)_Y$, $\mathrm{SU}(2)_L$, and $\mathrm{SU}(3)_C$ gauge fermions.

In the minimal SUGRA model the soft SUSY-breaking terms are assumed to take the following universal structures at the GUT scale:

$$\begin{gathered}(m_Q^2)_{ij}=(m_U^2)_{ij}=(m_D^2)_{ij}=m_0^2\delta_{ij},\\(m_L^2)_{ij}=(m_E^2)_{ij}=m_0^2\delta_{ij},\\\Delta_1^2=\Delta_2^2=m_0^2,\\A_{Uij}=f_{Uij}A_X,\quad A_{Dij}=f_{Dij}A_X,\quad A_{Eij}=f_{Eij}A_X,\\m_{\tilde{B}}=m_{\tilde{W}}=m_{\tilde{G}}=M_{gX}.\end{gathered} \tag{2.4}$$

With this initial condition, soft SUSY-breaking parameters at the electroweak scale are calculated by solving the RGE's of the MSSM [12]. We first solve the one-loop RGE's for the gauge coupling constants taking $\alpha_i(m_Z)$ as the input and determine the GUT scale, M_{GUT}, where the gauge couplings meet. The Yukawa coupling constants at M_{GUT} are also calculated by solving the RGE's from m_Z to M_{GUT}. The values of the Yukawa coupling constants at the electroweak scale are obtained by taking the quark-lepton masses, the Cabbibo-Kobayashi-Maskawa (CKM) matrix elements, and the $\tan\beta=\langle h_2^0\rangle/\langle h_1^0\rangle$ as input parameters. Then we solve the RGE's for all MSSM parameters downward with the GUT scale boundary conditions (2.4) for each set of the universal soft SUSY-breaking parameters (m_0,A_X,M_{gX}). We include all generation mixings in the RGE's for both Yukawa coupling constants and the soft SUSY-breaking parameters. Next, we evaluate the Higgs potential at the electroweak scale and require that the minimum of the potential gives a correct vacuum expectation values of the neutral Higgs fields as $\langle h_1^0\rangle=v\cos\beta$ and $\langle h_2^0\rangle=v\sin\beta$ where $v=174$ GeV. This is known as the radiative electroweak symmetry-breaking scenario [11]. The effective potential of neutral Higgs fields at the electroweak scale is given by

$$V(h_1^0,h_2^0)=(\mu^2+\Delta_1^2)|h_1^0|^2+(\mu^2+\Delta_2^2)|h_2^0|^2 + (B\mu h_1^0 h_2^0+\text{H.c.})+\frac{g^2+g'^2}{8}(|h_1^0|^2-|h_2^0|^2)^2 + V_{\text{loop}}, \tag{2.5}$$

where V_{loop} is the one-loop correction induced by the third-generation fermions and sfermions [10]. The requirement of the radiative electroweak symmetry-breaking determines the magnitude of the SUSY Higgs mass parameter μ and the soft SUSY-breaking parameter B. The explicit forms of V_{loop} and the condition of the radiative electroweak symmetry breaking used in the present analysis are given in Appendix A. At this stage, all MSSM parameters at the electroweak scale are determined as functions of the input parameters [$\tan\beta$, m_0, A_X, M_{gX}, $\text{sgn}(\mu)$].

With use of the low-energy SUSY parameters determined by the procedure described above, we can calculate all the SUSY particle masses and the mixing parameters. The 6×6 mass matrix of the up-type squark is written by

$$-\mathcal{L}=(\tilde{u}_L^*,\tilde{u}_R^*)M_{\tilde{u}}^2\begin{pmatrix}\tilde{u}_L\\ \tilde{u}_R\end{pmatrix} =(\tilde{u}_{Li}^*,\tilde{u}_{Ri}^*)\begin{pmatrix}(m_{LL}^2)_{ij} & (m_{LR}^2)_{ij}\\ (m_{RL}^2)_{ij} & (m_{RR}^2)_{ij}\end{pmatrix}\begin{pmatrix}\tilde{u}_{Lj}\\ \tilde{u}_{Rj}\end{pmatrix}, \tag{2.6}$$

$$(m_{LL}^2)_{ij}=(M_U^\dagger M_U)_{ij}+(m_Q^2)_{ij} + m_Z^2\cos(2\beta)\left(\frac{1}{2}-\frac{2}{3}\sin^2\theta_W\right)\delta_{ij}, \tag{2.7}$$

$$(m_{RR}^2)_{ij}=(M_U M_U^\dagger)_{ij}+(m_U^2)_{ij}+m_Z^2\cos(2\beta)\left(\frac{2}{3}\sin^2\theta_W\right)\delta_{ij}, \tag{2.8}$$

$$(m_{LR}^2)_{ij}=(m_{RL}^{2\dagger})_{ij}=-\mu\ \cot\beta(M_U^\dagger)_{ij}+(A_U^*)_{ij}v\ \sin\beta, \tag{2.9}$$

where M_U is the up-type quark mass matrix, i.e., $M_{Uij}=f_{Uji}v\ \sin\beta$, and $\tilde{u}_L$ is the up-type component of the SU(2) doublet $\tilde{q}$. In this weak eigenstate, the mass matrix is not diagonal at the electroweak scale. The physical mass eigenstate is given by diagonalizing the mass matrix:

$$\tilde{u}_I=(\tilde{U}_U)_I^J\begin{pmatrix}\tilde{u}_L\\ \tilde{u}_R\end{pmatrix}_J, \tag{2.10}$$

$$\tilde{U}_U(M_{\tilde{u}}^2)\tilde{U}_U^\dagger=\text{diagonal}, \tag{2.11}$$

where $\tilde{u}_I$ is the mass eigenstate. The unitary matrix $\tilde{U}_U$ induces new flavor mixing in the up-type squark sector. In a similar manner, we define the mixing matrices $\tilde{U}_D$, $\tilde{U}_l$ for the down-type squark and the slepton sectors.

III. $b\to sl^+l^-$ DECAY

In this section, we describe the calculation of the branching ratio and the lepton forward-backward asymmetry for the $b\to sl^+l^-$ ($l=e,\mu$) process in the minimal SUGRA model. We first introduce the effective Hamiltonian which is relevant for the $b\to sl^+l^-$ process [13]:

$$H_{\text{eff}}=\frac{4G_F}{\sqrt{2}}\sum_{i=1}^{10}C_i(Q)O_i(Q), \tag{3.1}$$

where Q is the renormalization point. For the calculation of the branching ratio, the following three operators are important:

$$O_7=\frac{e}{16\pi^2}\,m_b(\bar{s}_{L\alpha}\sigma_{\mu\nu}b_{R\alpha})F^{\mu\nu}, \tag{3.2}$$

$$O_9=\frac{e^2}{16\pi^2}\,(\bar{s}_{L\alpha}\gamma_\mu b_{L\alpha})(\bar{l}\gamma^\mu l), \tag{3.3}$$

$$O_{10}=\frac{e^2}{16\pi^2}\,(\bar{s}_{L\alpha}\gamma_\mu b_{L\alpha})(\bar{l}\gamma^\mu\gamma_5 l). \tag{3.4}$$

The explicit forms of all the effective operators $O_i(Q)$ are given in Appendix B. Throughout this paper we neglect the strange quark mass.

The coefficients $C_1(m_W)-C_{10}(m_W)$ are determined by matching the full theory with the effective theory at the renormalization point $Q=m_W$. The coefficients $C_1(m_W)-C_6(m_W)$ are given by

$$C_2(m_W)=-\lambda_t,\quad C_i(m_W)=0\quad (i=1,3\text{–}6), \tag{3.5}$$

where $\lambda_t=V_{tb}V_{ts}^*$. Note that there is no SUSY contribution to these values at the tree level. The coefficients $C_7(m_W)-C_{10}(m_W)$ are generated by one-loop diagrams. In order to determine these coefficients at the m_W scale, we need to calculate photon penguin, Z penguin, and box diagrams taking account of new contributions in addition to the SM diagrams. There are four classes of new contributions in the SUSY model: charged Higgs boson (H^-), up-type quark

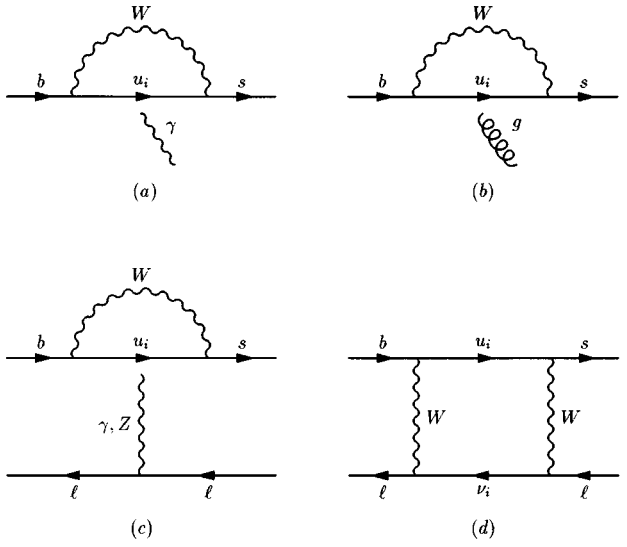

FIG. 1. Feynman diagrams in the SM. (a) $b\to s\gamma$, (b) $b\to sg$, (c) the penguin diagram for $b\to sl^+l^-$, (d) box diagram for $b\to sl^+l^-$. The SUSY contributions to these diagrams are obtained by replacing the internal lines with SUSY particles.

loop; chargino ($\widetilde{x}^-$) up-type squark loop; gluino ($\widetilde{G}$), down-type squark loop; and neutralino ($\widetilde{x}^0$) down-type squark loop. $C_7(m_W)$ is obtained by calculating the photon penguin diagram Fig. 1(a). $C_8(m_W)$ is also obtained by calculating the gluon penguin diagram Fig. 1(b). There are three types of diagrams which contribute to $C_9(m_W)$: the photon penguin diagram, Fig. 1(c); the Z penguin diagram, Fig. 1(c); and the box diagram, Fig. 1(d). Since we neglect the lepton mass, there is no charged Higgs contribution to the box diagram. $C_{10}(m_W)$ is induced by the Z penguin diagram, Fig. 1(c), and the box diagram, Fig. 1(d). The explicit form of each contribution is given in Appendix C with use of the mixing matrices at each vertex defined in Appendix D and Inami-Lim functions given in Appendix E.

In order to calculate the $b\to s l^+ l^-$ decay amplitude, we need the effective Hamiltonian at the m_b scale. By solving the RGE's in the leading logarithmic approximation (LLA) of QCD, $C_i(m_b)$ can be related with $C_i(m_W)$ as given in Appendix F [14]. With this effective Hamiltonian at the m_b scale, we can calculate various physical observables. Since the bottom quark is much heavier than the QCD energy scale, we can calculate the inclusive decay width as a free bottom quark decay. This procedure is justified as a leading-order approximation of the heavy quark expansion [15]. The $b\to s l^+ l^-$ branching ratio is given by

$$\frac{dB(b\to s l^+ l^-)}{d\hat{s}} = B(b\to c e \overline{\nu})\,\frac{\alpha^2}{4\pi^2}\left|\frac{1}{V_{cb}}\right|^2 \frac{1}{f_{\rm ph}(m_c/m_b)}\, w(\hat{s})\sqrt{1-\frac{4m_l^2}{s}}\left(|C_9+Y(\hat{s})|^2\alpha_1(\hat{s},\hat{m}_s,\hat{m}_l)+|C_{10}|^2\alpha_2(\hat{s},\hat{m}_s,\hat{m}_l)\right.$$
$$\left.+\frac{4}{\hat{s}}|C_7|^2\alpha_3(\hat{s},\hat{m}_s,\hat{m}_l)+12\alpha_4(\hat{s},\hat{m}_s,\hat{m}_l)\mathrm{Re}\{C_7^*[C_9+Y(\hat{s})]\}\right), \tag{3.6}$$

where $\hat{s}=(p_+ + p_-)^2/m_b^2$ and $p_+(p_-)$ is the four-momentum of $l^+(l^-)$. Here we normalize the branching ratio by the semileptonic branching ratio $B(b\to c e\overline{\nu})$ in order to cancel the m_b^5 factor in the differential width. The function $f_{\rm ph}(x)=1-8x^2+8x^6-x^8-24x^4\ln x$ is the phase-space factor of the semileptonic decay width. Kinematical functions $\alpha_1-\alpha_4$ and $w(\hat{s})$ are given in Appendix G. As mentioned before we neglect the strange quark mass in the numerical analysis. The lepton mass, is, however, kept since lepton mass corrections are important in the lower end of the lepton invariant mass spectrum. By calculating the matrix elements of four quark operators O_1-O_6 at the one-loop level, we obtain $Y(\hat{s})$

$$Y(\hat{s}) = g\left(\frac{m_c}{m_b},\hat{s}\right)(3C_1+C_2+3C_3+C_4+3C_5+C_6) - \frac{1}{2}g(1,\hat{s})(4C_3+4C_4+3C_5+C_6) - \frac{1}{2}g(0,\hat{s})(C_3+3C_4) + Y_{\rm res}(\hat{s}), \tag{3.7}$$

$$g(z,\hat{s}) = \begin{cases} -\frac{4}{9}\ln z^2 + \frac{8}{27} + \frac{16z^2}{9\hat{s}} - \frac{2}{9}\sqrt{1-\frac{4z^2}{\hat{s}}}\left(2+\frac{4z^2}{\hat{s}}\right)\left(\ln\left|\frac{1+\sqrt{1-\frac{4z^2}{\hat{s}}}}{1-\sqrt{1-\frac{4z^2}{\hat{s}}}}\right| - i\pi\right) & \text{for } \hat{s}>4z^2, \\ -\frac{4}{9}\ln z^2 + \frac{8}{27} + \frac{16z^2}{9\hat{s}} - \frac{4}{9}\sqrt{\frac{4z^2}{\hat{s}}-1}\left(2+\frac{4z^2}{\hat{s}}\right)\arctan\left(\frac{1}{\sqrt{\frac{4z^2}{\hat{s}}-1}}\right) & \text{for } \hat{s}<4z^2. \end{cases} \tag{3.8}$$

In addition to these short-distance contributions, there are long-distance contributions from the $c\overline{c}$ resonances, $b\to s J/\psi\to l^+ l^-$ and $b\to s\psi'\to l^+ l^-$. Although we can avoid large contributions from these resonances by cutting the resonance regions of the lepton-invariant-mass spectrum, there can be sizable effects from interference between the short-distance contribution and the tail of the resonances. The resonance effects in the $b\to s$ transition have been investigated in connection to the long-distance contribution of the $b\to s l^+ l^-$ [16–18] as well as the $b\to s\gamma$ [19] process. In Eq. (3.7) following [16,17] we have introduced the resonance term $Y_{\rm res}(\hat{s})$

$$Y_{\rm res}(\hat{s}) = \kappa\,\frac{3\pi}{\alpha^2}\sum_{i=J/\psi,\psi'}\frac{M_i\Gamma(i\to l^+ l^-)/m_b^2}{\hat{s}-M_i^2/m_b^2+iM_i\Gamma_i/m_b^2}, \tag{3.9}$$

where κ parametrizes the b-s-J/ψ and b-s-ψ' couplings. Its absolute value is determined from $\Gamma(b\to J/\psi X)$ and is given by $|\kappa|\sim 1$ [16,17]. In general, κ can have a nonzero phase. In the following, in order to see the effect of the phase, we show results with[1] $\kappa=\pm 1$. In the actual evaluation of the branching ratio the charm mass in Eq. (3.7) is taken to be the D meson mass [16]. The choice of the charm mass is not important here since the branching ratio depends on it very weakly.

[1] In principle, κ can be different for J/ψ and ψ'. But for simplicity, we take the same value in Eq. (3.9). From the experimental data at least we can show that the absolute value is almost the same both for J/ψ and ψ'.

Another observable which is expected to be measured with reasonable accuracy in future experiments is the forward-backward asymmetry of the lepton [17]. In the center-of-mass frame of the lepton pair, this is defined as

$$\mathcal{A}_{\rm FB}(\hat{s}) = \frac{\int_0^1 d(\cos\theta)[d^2B/d(\cos\theta)d\hat{s}](b\to s l^+ l^-) - \int_{-1}^0 d(\cos\theta)[d^2B/d(\cos\theta)d\hat{s}](b\to s l^+ l^-)}{\int_0^1 d(\cos\theta)[d^2B/d(\cos\theta)d\hat{s}](b\to s l^+ l^-) + \int_{-1}^0 d(\cos\theta)[d^2B/d(\cos\theta)d\hat{s}](b\to s l^+ l^-)}$$
$$= -\frac{3w(\hat{s})\sqrt{1-4\hat{m}_l^2/\hat{s}}C_{10}\{\hat{s}[C_9+\mathrm{Re}\ Y(\hat{s})]+2C_7\}}{\{|C_9+Y(\hat{s})|^2\alpha_1+C_{10}^2\alpha_2+(4/\hat{s})C_7^2\alpha_3+12\alpha_4 C_7[C_9+\mathrm{Re}\ Y(\hat{s})]\}}, \tag{3.10}$$

where θ is the angle between the momentum of the bottom quark and that of the l^+.

IV. NUMERICAL RESULTS

As explained in Sec. II, the MSSM parameters are determined by solving the RGE's. In the minimal SUGRA model, there are five SUSY parameters; the universal scalar mass m_0, the gaugino mass M_{gX}, the universal A parameter A_X, the SUSY-invariant. Higgs boson mass μ, the mixing parameter of Higgs boson B. Using the condition that the electroweak symmetry is properly broken to give the correct Z boson mass, the theory contains four free parameters, $\tan\beta$, m_0, M_{gX}, and A_X as well as the sign of μ. We scan the parameters m_0, M_{gX}, and A_X in the range of $m_0 \leqslant 2$ TeV, $M_{gX} \leqslant 2$ TeV, and $|A_X| \leqslant 5m_0$ for each fixed value of $\tan\beta$. We also impose the following phenomenological constraints.

(1) $b\to s\gamma$ branching ratio. The branching ratio of the $b\to s\gamma$ process is given by

$$B(b\to s\gamma) = \frac{6\alpha}{\pi}\left|\frac{1}{V_{cb}}\right|^2 B(b\to ce\overline{\nu})|C_7(Q)|^2. \tag{4.1}$$

Most important theoretical ambiguity comes from the choice of the renormalization scale Q. The branching ratio changes by about $\pm 30\%$ as the scale Q is varied in the range of $m_b/2 \leqslant Q \leqslant 2m_b$. We fix $Q = m_b$ in this analysis and discuss the ambiguity associated to the QCD correction later. From the measurement by CLEO [1], the inclusive branch ratio is given by

$$1\times 10^{-4} < B(b\to s\gamma) < 4.2\times 10^{-4}. \tag{4.2}$$

(2) From the recent experiment at LEP 1.5 [20], we impose that all the charged SUSY particles are heavier than 65 GeV.

(3) All sneutrino masses are larger than 41 GeV [21].

(4) The gluino mass is larger than 100 GeV. The lower bound of the experimental gluino mass is given by Fermilab Tevatron collider [22]. Since it depends on various SUSY parameters, we take 100 GeV as a conservative lower bound.[2]

(5) From the neutralino search at the CERN e^+e^- collider LEP [23], we impose

$$\Gamma(Z\to\chi\chi) < 8.4\ \mathrm{MeV}, \tag{4.3}$$

$$B(Z\to\chi\chi'), B(Z\to\chi'\chi') < 2\times 10^{-5}, \tag{4.4}$$

where χ is the lightest neutralino and χ' denotes another neutralino.

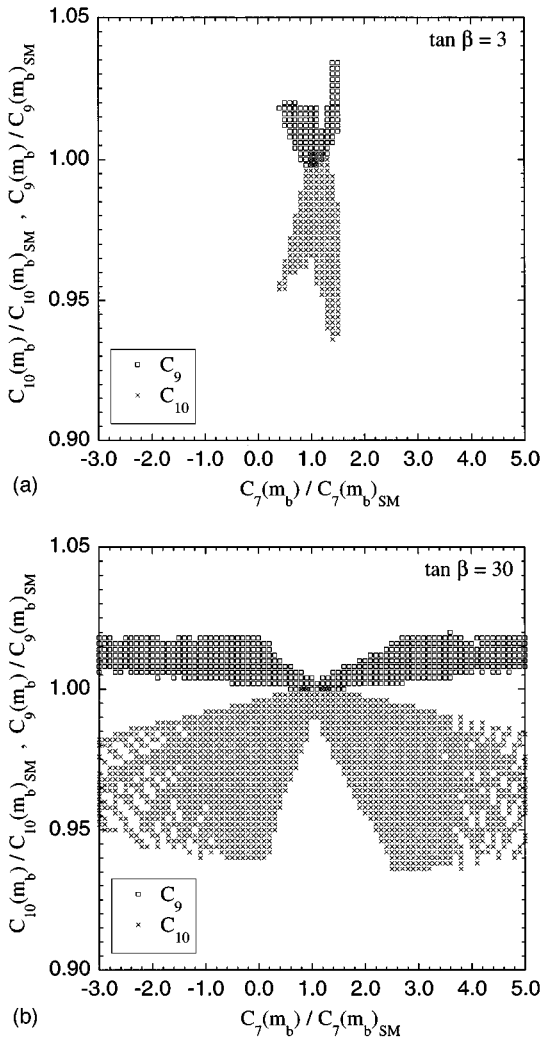

FIG. 2. $C_7(m_b)$, $C_9(m_b)$, and $C_{10}(m_b)$ in the SUGRA model normalized to that of in the SM (a) for $\tan\beta = 3$ and (b) for $\tan\beta = 30$.

[2]With use of the GUT relation of the gaugino masses Eq. (2.4) and the LEP 1/1.5 constraints on charginos and neutralinos (above 2 and 5), a gluino lighter than about 150 GeV is excluded for $\tan\beta \gtrsim 2$. Therefore the precise value of the imposed gluino mass bound is not very important.

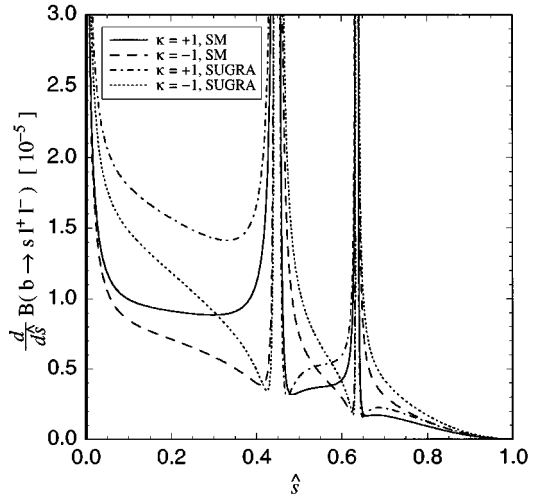

FIG. 3. $B(b\to sl^+l^-)$ in the SM and in the minimal SUGRA model for $\kappa=\pm1$. The SUSY parameters are fixed with $\tan\beta=30$, $m_0=369$ GeV, $M_{gX}=100$ GeV, $A_X=m_0$, where $C_7(m_b)$ becomes the opposite sign to the SM.

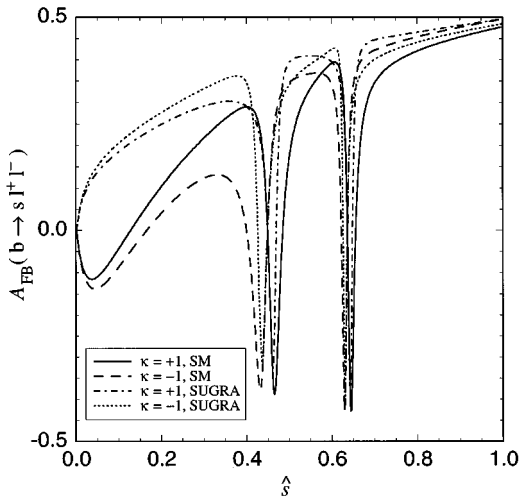

FIG. 4. $\mathcal{A}_{\rm FB}(b\to sl^+l^-)$ in the SM and in the minimal SUGRA model for $\kappa=\pm1$. The SUSY parameters are fixed with $\tan\beta=30$, $m_0=369$ GeV, $M_{gX}=100$ GeV, $A_X=m_0$, where $C_7(m_b)$ becomes the opposite sign to the SM.

(6) The lightest SUSY particle is neutral.

(7) The condition for not having a charge or color symmetry-breaking vacuum [24].

Throughout this paper we fix the top-quark mass as 175 GeV, the bottom-quark pole mass as 4.62 GeV and $\alpha_{s(m_Z)}=0.116$. In Fig. 2, we show $C_7(m_b)$, $C_9(m_b)$, and $C_{10}(m_b)$, each of which is normalized to its SM value, for $\tan\beta=3$, 30. In these figures we do not include the $b\to s\gamma$ constraint. We can see that in Fig. 2, $C_7(m_b)$ can be quite different from the SM value and even the opposite sign is allowed for $\tan\beta=30$. On the other hand, $C_9(m_b)$ and $C_{10}(m_b)$ differ from the SM values by at most 5% in the whole parameter space for both $\tan\beta=3$, 30. In the calculation of $C_7(m_b)$, there is a one-loop diagram with internal stop and chargino which gives a large contribution when $\tan\beta$ becomes large [6]. When chargino has a sizable Higgsino component, this diagram is proportional to the product of the top and bottom Yukawa coupling constants, i.e., $m_t m_b/(\sin\beta\cos\beta)$, which grows as $\tan\beta$ when $\tan\beta$ is large. On the other hand, there are no such terms in the calculation of $C_9(m_b)$ and $C_{10}(m_b)$. In fact, the corresponding stop-Higgsino diagram in $C_9(m_b)$ and $C_{10}(m_b)$ is proportional to the square of the top Yukawa coupling constants, namely $m_t^2/\sin^2\beta$, which does not grow for large $\tan\beta$. Indeed $C_9(m_b)$ and $C_{10}(m_b)$ could be large if $\tan\beta\leqslant1$, but within the framework of the minimal SUGRA model $\tan\beta$ is only allowed to be larger than two as far as we require that the top Yukawa coupling constant remains perturbative up to the GUT scale.

We first show our numerical results for $b\to s\mu^+\mu^-$ and discuss the electron case later. In Figs. 3 and 4, the branching ratio and the forward-backward asymmetry in the SM are shown as functions of the lepton pair invariant mass. In the calculation of the $b\to sl^+l^-$ branching ratio we have used $m_c/m_b=0.31$, $|V_{cb}/\lambda_t|=1.01$, and $B(b\to ce\overline{\nu})=0.104$ in Eq. (3.6). We also show similar curves for the minimal SUGRA model with a particular set of parameters that $\tan\beta=30$, $m_0=369$ GeV, $M_{gX}=100$ GeV, $A_X=m_0$ and the sign of μ is positive. This parameter set is chosen so that $C_7(m_b)$ has the same magnitude but the opposite sign to the SM value. We show the curves with $\kappa=\pm1$ for both models. As can be seen in Figs. 3 and 4, there are large contributions from the J/ψ and ψ' resonances. Since we are interested only in the short-distance contribution, we consider the following two regions: the low-s region, $4m_l^2<s<(m_{J/\psi}-\delta)^2$, and the high-$s$ region, $(m_{\psi'}+\delta)^2<s<m_b^2$, where δ is introduced to cut the resonance regions and we take $\delta=100$ MeV here. We can see that the sizable interference between the long- and short-distance contributions even in these low- and high-s regions. At the asymmetric B factory experiments, however, it may be possible to determine the phase of κ by measuring the lepton invariant spectrum near the resonance regions. Therefore, in the following, we consider the branching ratio and asymmetry integrated in the above two kinematical regions with a choice of $\kappa=\pm1$. These are defined as

$$B^{\rm low(high)}=\int_{\rm low(high)}d\hat{s}B(\hat{s}), \tag{4.5}$$

$$\mathcal{A}_{\rm FB}^{\rm low(high)}=\frac{\int_{\rm low(high)}d\hat{s}\left(\int_0^1 d(\cos\theta)[d^2B/d(\cos\theta)d\hat{s}]-\int_{-1}^0 d(\cos\theta)[d^2B/d(\cos\theta)d\hat{s}]\right)}{\int_{\rm low(high)}d\hat{s}\left(\int_0^1 d(\cos\theta)[d^2B/d(\cos\theta)d\hat{s}]+\int_{-1}^0 d(\cos\theta)[d^2B/d(\cos\theta)d\hat{s}]\right)}. \tag{4.6}$$

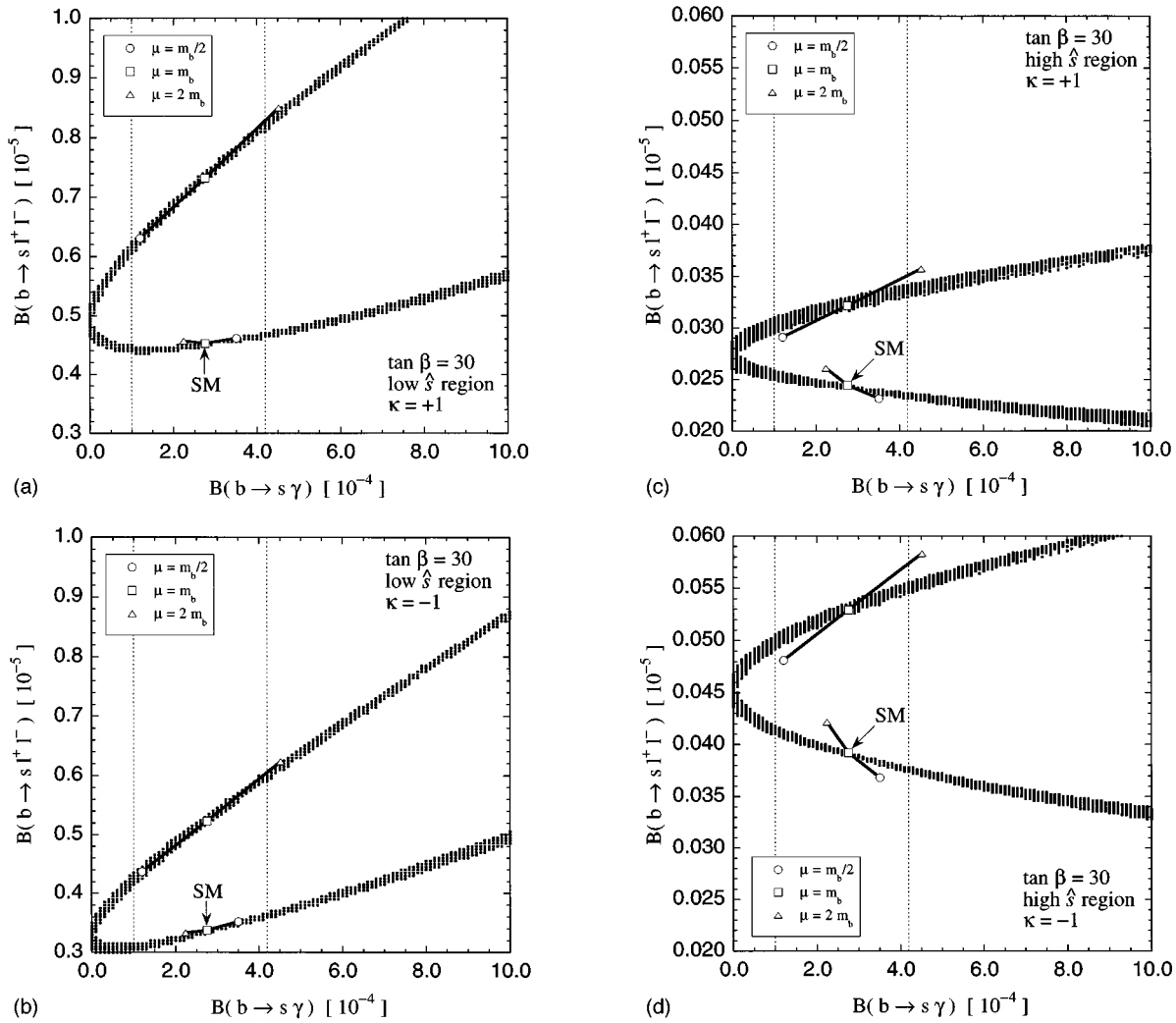

FIG. 5. A correlation between $B(b\to s\gamma)$ and $B(b\to sl^+l^-)$ in the minimal SUGRA model (a) in the low-s region with $\kappa=+1$, (b) in the low-s region with $\kappa=-1$, (c) in the high-s region with $\kappa=+1$, and (d) in the high-s region with $\kappa=-1$ for $\tan\beta=30$. Two vertical dashed lines represent the experimental $b\to s\gamma$ constraint. Circles, squares, and triangles represent how much $B(b\to s\gamma)$ and $B(b\to sl^+l^-)$ change when the renormalization point Q is taken to be $m_b/2$, m_b, and $2m_b$, respectively.

Notice that for general phase of κ the branching ratio takes the value between the $\kappa=\pm1$ cases.

In Fig. 5, we show the correlation between the branching ratios of the $b\to s\gamma$ and $b\to sl^+l^-$ in the above two regions for $\tan\beta=30$. Figures 5(a) and 5(b) show the branching ratio of $b\to sl^+l^-$ in the low-s region for $\kappa=\pm1$, and Figs. 5(c) and 5(d) correspond to the high-s region. As already mentioned in connection with Fig. 2, only $C_7(m_b)$ can receive sizable SUSY contributions. It is therefore clear from Eq. (4.1) and Eq. (3.6) that the values of two branching ratios lie on a parabola when we neglect the SUSY contribution to $C_9(m_b)$ and $C_{10}(m_b)$. This is seen in Fig. 5. If we take the experimental constraint on the branching ratio of $b\to s\gamma$ into account, two separate regions are allowed. One corresponds to the case when the sign of $C_7(m_b)$ is the same as that of the SM, and the other corresponds to the case with the opposite sign. We can see that the branching ratio of $b\to sl^+l^-$ is enhanced about 50% in the latter case. Although the branching ratio of $b\to sl^+l^-$ in the low-s region changes $\pm15\%$ depending on the sign of κ, we can distinguish the sign of $C_7(m_b)$ from the branching ratio integrated in this region. On the other hand, in the high-s region, the branching ratio of $b\to sl^+l^-$ depends on the sign of κ significantly.

We also show the correlations between the branching ratio of the $b\to s\gamma$ and the forward-backward asymmetry of the $b\to sl^+l^-$ in Fig. 6. Four figures correspond to the case $\kappa=\pm1$ and low-high regions. We can see that the asymmetry is also useful to distinguish the sign of $C_7(m_b)$.

We vary the renormalization point Q from $m_b/2$ to $2m_b$ in order to study the renormalization point dependences, which are also shown in Figs. 5 and 6. We see that the tendency is that the branching ratio changes along the parabola. This is because the change of the renormalization point Q mainly affects $C_7(Q)$. This means that we can make a prediction of the branching ratio of $b\to sl^+l^-$ without much ambiguity as far as we use the experimental value of the $b\to s\gamma$ branching ratio.[3] Figure 7 shows that the branching ratio of $b\to sl^+l^-$ in the low-s region as a function of the chargino mass and

[3]It is important, however, to reduce the ambiguity of the renormalization point in order to put constraints on SUSY parameter space from the $b\to s\gamma$ branching ratio.

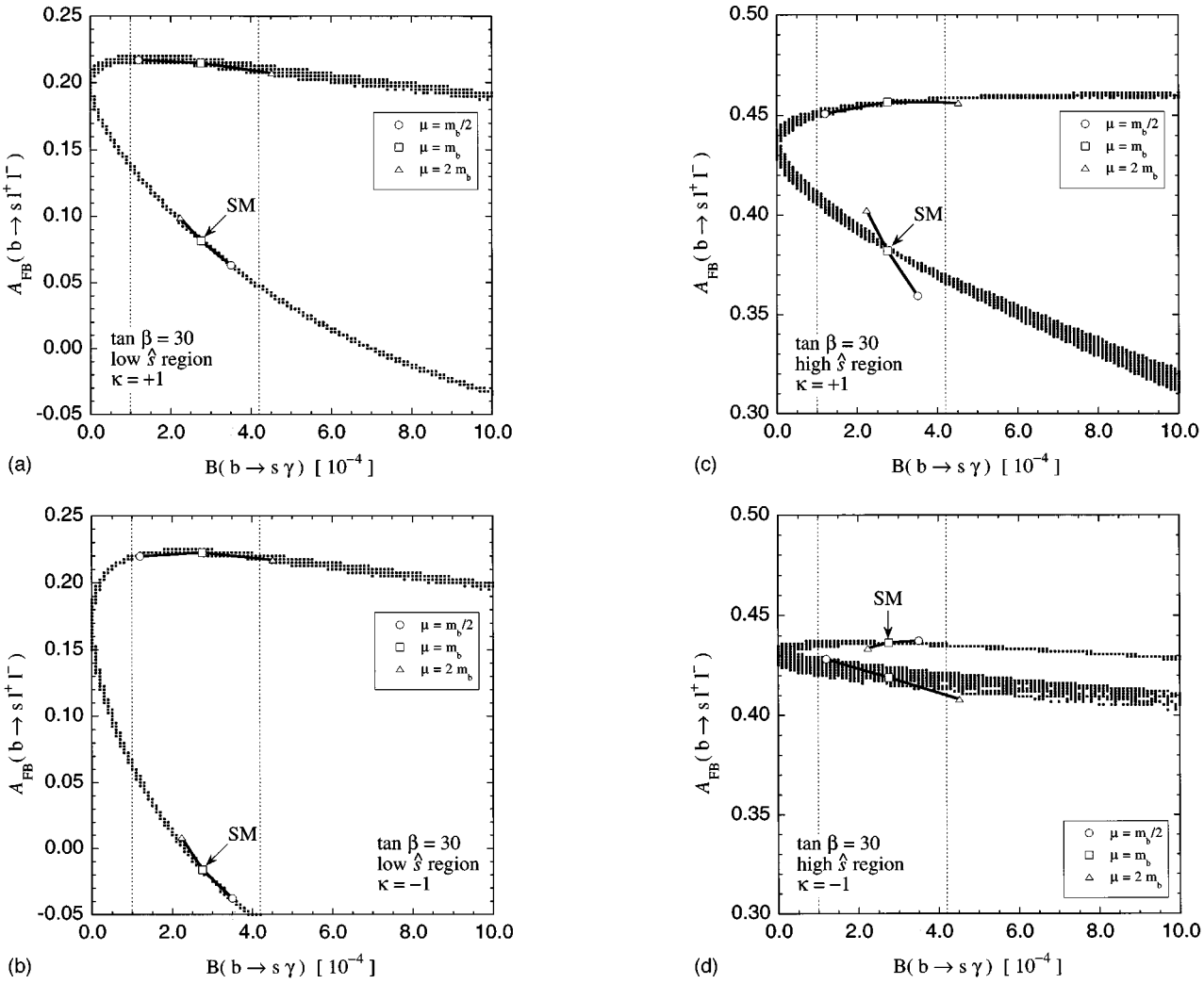

FIG. 6. A correlation between $B(b\to s\gamma)$ and $\mathcal{A}_{\rm FB}(b\to sl^+l^-)$ in the minimal SUGRA model (a) in the low-s region with $\kappa=+1$, (b) in low-s region with $\kappa=-1$, (c) in the high-s region with $\kappa=+1$, and (d) in the high-s region with $\kappa=-1$ for $\tan\beta=30$. Two vertical dashed lines represent the experimental $b\to s\gamma$ constraint. Circles, squares, and triangles represent how much $B(b\to s\gamma)$ and $\mathcal{A}_{\rm FB}(b\to sl^+l^-)$ change when the renormalization point Q is taken to be $m_b/2$, m_b, and $2m_b$, respectively.

the light stop mass for $\kappa=1$ and $\tan\beta=30$ taking account of the $b\to s\gamma$ constraint. The points where the branching ratio of the $b\to sl^+l^-$ is enhanced about 50% compared to the SM correspond to the case that the $C_7(m_b)$ has the opposite sign to the SM. It is interesting to see such parameters correspond to relatively light SUSY particles ($m_{\chi^-}\lesssim 130$ GeV, $m_{\tilde{t}}\lesssim 250$ GeV) but beyond the reach of LEP II. We have also analyzed the case of small $\tan\beta$, for example, $\tan\beta=3$. In this case the $C_7(m_b)$ cannot change its sign as shown in Fig. 2, thus the branching ratios change within $\pm 5\%$ after taking into the account the $b\to s\gamma$ constraint.

We also calculated the branching ratio and the asymmetry for the $b\to se^+e^-$ process. The only difference from the $b\to s\mu^+\mu^-$ case is that the lower limit of the lepton invariant mass becomes smaller. Since the $C_7(m_b)$ term gives dominant contribution in the region near the kinematical lower limit, the branching ratio and asymmetry integrated in the low-s region change from those for $b\to s\mu^+\mu^-$. Compared to Fig. 5(a), for example, the $b\to se^+e^-$ branching ratio is enhanced by $\sim 5\%$ at $B(b\to s\gamma)=1.0\times 10^{-4}$ and $\sim 30\%$ at $B(b\to s\gamma)=4.2\times 10^{-4}$ for the SM branch and by ~ 5 and $\sim 2\,\%$, respectively, for the branch with opposite sign of $C_7(m_b)$. It is worthwhile noting that we can distinguish the sign of $C_7(m_b)$ by looking at the low-s region in the $b\to se^+e^-$ mode just as in the $b\to s\mu^+\mu^-$ case. On the other hand, the branching ratio and asymmetry integrated in the high-s region do not change noticeably from the $b\to s\mu^+\mu^-$ case.

Let us now compare our results with those in [9]. As explained in Sec. II, we have included the one-loop correction term $V_{\rm loop}$ in the Higgs potential to find appropriate parameter sets. This correction, however, mainly affects the mass of the lightest neutral Higgs boson, which does not directly contribute to the FCNC processes. Consequently the effect of this improvement is rather small.[4] The most important difference comes from the long-distance contributions of the $c\bar{c}$ resonances. In [9], $b\to sl^+l^-$ branching ratio is cal-

[4]The effect on the lightest Higgs boson mass will be important in finding allowed SUSY parameter regions when the experimental bound of the lightest Higgs boson mass is raised.

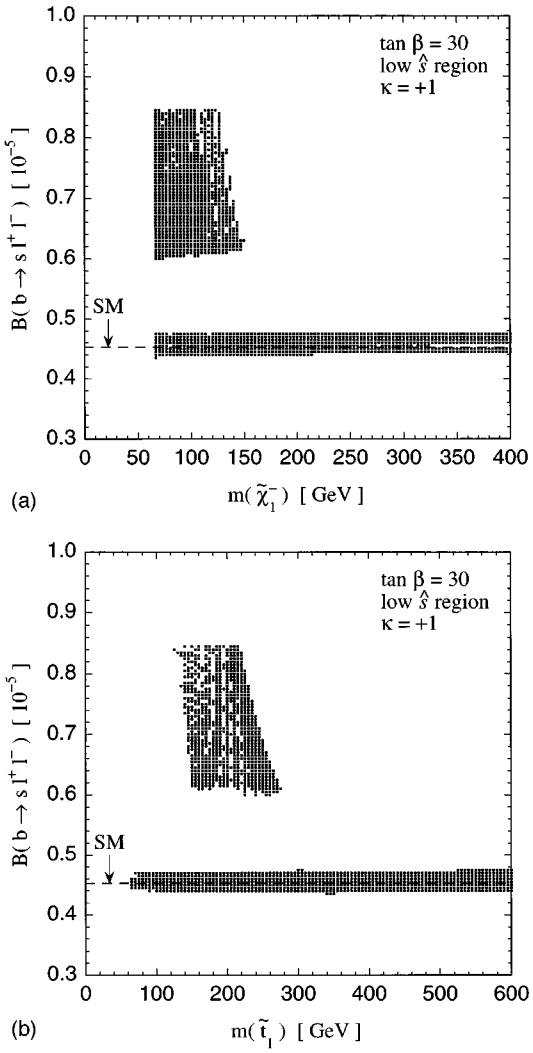

FIG. 7. $B(b\to sl^+l^-)$ in the low-s region for $\tan\beta=30$ as a function of (a) the light chargino mass and (b) the light top squark mass. The solid line shows the value in the SM.

culated with the short-distance contributions only, omitting the J/ψ and ψ' resonance regions from the integration range of the lepton pair invariant mass. We show that even if the resonance regions are avoided, the interference effect between the short-distance contributions and the tail of the resonances gives $\sim\pm 15\%$ ambiguity to the $b\to sl^+l^-$ branching ratio since the detail of the b-s-J/ψ and b-s-ψ' couplings, which are parametrized by the phase of κ in our present analysis, is theoretically unknown. We see that this ambiguity is larger than the short-distance effects from the SUSY contributions unless C_7 changes its sign. Thus, it is difficult to extract information about the SUSY parameters from the branching ratio and the forward-backward asymmetry of $b\to sl^+l^-$ without knowledge of the long-distance contributions. This ambiguity will be reduced experimentally by the measurement of the behavior of the lepton pair invariant mass spectrum around the resonances. This may be achieved before the branching ratio in the off-resonance regions is measured since a large number of events is expected near the resonance regions.

V. $b\to s\nu\bar{\nu}$ DECAY

In this section, we present the numerical result of the branching ratio of $b\to s\nu\bar{\nu}$ in the minimal SUGRA model. For the calculation of this branching ratio, we need to introduce a new operator to the effective Hamiltonian Eq. (3.1):

$$O_{11}=\frac{g^2}{16\pi^2}(\bar{s}_{L\alpha}\gamma_\mu b_{L\alpha})\sum_{i=e,\mu,\tau}[\bar{\nu}_i\gamma^\mu(1-\gamma_5)\nu_i]. \tag{5.1}$$

The corresponding Wilson coefficient C_{11} is given in Appendix C. Note that C_{11} does not receive QCD correction in the leading logarithm approximation (LLA). In addition to the SM contribution, there are the Z penguin and the box diagrams due to the charged Higgs boson and SUSY particles. Since the effect of τ lepton mass in the loop diagram is small, C_{11} is calculated with three massless charged leptons. An important difference from the $b\to sl^+l^-$ process is that no photon penguin diagram can contribute to the $b\to s\nu\bar{\nu}$ process. Thus SUSY contributions to C_{11} are similar to those to C_{10}, and no large SUSY contribution is induced. The branching ratio of $b\to s\nu\bar{\nu}$ is written as

$$\sum_{i=e,\mu\tau}B(b\to s\nu_i\bar{\nu_i}) = 3B(b\to e\bar{\nu})\frac{\alpha_W^2}{4\pi^2}\left|\frac{1}{V_{cb}}\right|^2\frac{1}{f_{\rm ph}(m_c/m_b)}|C_{11}|^2. \tag{5.2}$$

In Fig. 8 we show the scatter plot of the $b\to s\nu\bar{\nu}$ branching ratio and the chargino mass (the light stop mass). In this calculation we have taken into account all constraints (1)–(7) in Sec. IV. We see that the branching ratio does not exceed the SM value and the change is at most 10%. This result does not depend much on the value of $\tan\beta$.

VI. CONCLUSIONS

In this paper, we have extensively examined the $b\to sl\bar{l}$ branching ratio in the minimal SUGRA model. By scanning the three-dimensional space of the soft SUSY-breaking parameters m_0, M_{gX}, and A_X for various choices of $\tan\beta$, we have found that a parameter region, where the Wilson coefficient $C_7(m_b)$ receives a large SUSY contribution, is still allowed under the LEP 1.5 constraints provided that $\tan\beta$ is large. On the other hand, the SUSY contributions to the coefficients $C_9(m_b)$ and $C_{10}(m_b)$ are much smaller than the SM contributions in the whole allowed parameter space. Consequently, there is a strong correlation between the predicted values of the branching ratios of $b\to s\gamma$ and $b\to sl^+l^-$. Applying the measured bound of the $b\to s\gamma$ branching ratio, we have shown that the predicted values of the $b\to sl^+l^-$ branching ratio are separated in two branches for a large $\tan\beta$: one corresponds to the region where the sign of the $b\to s\gamma$ amplitude is the same as that in the SM and the other corresponds to the opposite sign. In the latter case, the $b\to sl^+l^-$ branching ratio becomes, at most, $\sim 50\%$ larger compared to the SM value. The forward-backward asymmetry is also significantly different from the SM in the same parameter region. Since $m_{\chi^-}\gtrsim 100$ GeV is allowed for such a parameter region, it is possible to observe a large

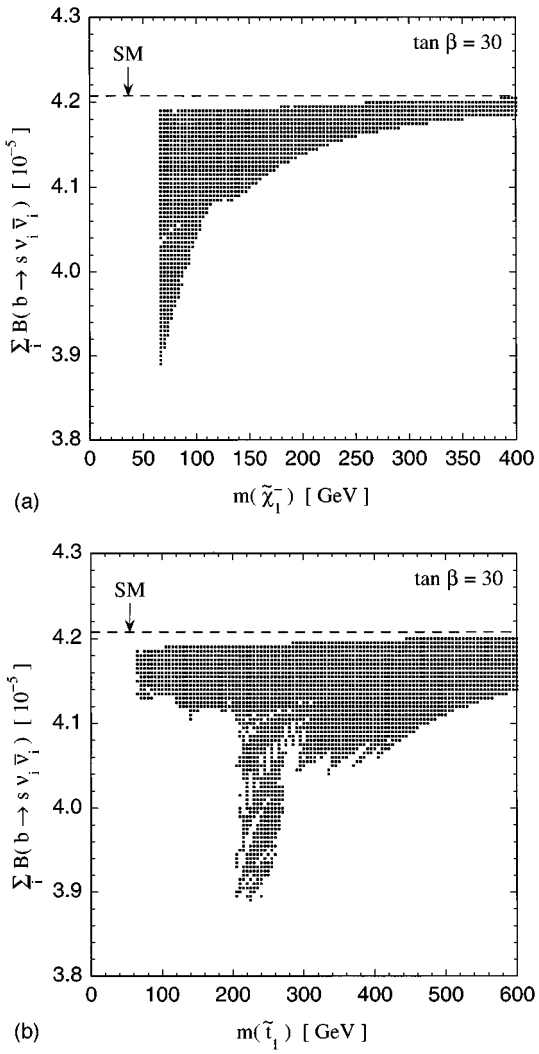

FIG. 8. $B(b\to s\nu\overline{\nu})$ for tanβ=30 as a function of (a) the light chargino mass and (b) the light top squark mass. The solid line shows the value in the SM.

enhancement in the branching ratio of $b\to sl^+l^-$ even if no SUSY particle is found at LEP II. We also calculated the branching ratio of $b\to s\nu\overline{\nu}$ process and found that it is reduced at most 10% from the SM value.

There are several theoretical ambiguities in the calculation of $b\to sl^+l^-$ branching ratio, such as the $c\overline{c}$ resonance effect, the renormalization point dependence, the strange quark mass, and the higher-order corrections in the heavy-quark expansion. Among them we studied the renormalization point dependence and the resonance effects in some detail. The strange quark mass correction, which is of order m_s^2/m_b^2, is estimated to be less important especially in the low-s region. The higher-order corrections in the heavy-quark expansion is also expected to be small [15].

The renormalization point dependence gives about 30% ambiguity to determine the magnitude of $C_7(m_W)$ from the measured value of $b\to s\gamma$ branching ratio. This ambiguity, however, does not affect the correlation between the branching ratios of $b\to s\gamma$ and $b\to sl^+l^-$ much. We can make a rather definite prediction on the value of the $b\to sl^+l^-$ branching ratio with use of the measured $b\to s\gamma$ branching ratio.

The $c\overline{c}$ resonance effect turns out to be important. To deal with this effect, we have introduced a phenomenological parameter κ and have presented our results for $\kappa=\pm1$ since the phase of κ is not known theoretically. We have pointed out that there are sizable ambiguities due to this effect for both low- and high-s regions. This ambiguity will be reduced experimentally if the lepton invariant mass spectrum near the resonances will be measured in some detail. We have also found that in the low-s region the change of the $b\to sl^+l^-$ branching ratio due to the sign of $C_7(m_b)$ is larger than the ambiguity induced from the phase of κ. This fact enables us to distinguish the sign of $C_7(m_b)$ without the knowledge of the phase of κ, by measuring the $b\to sl^+l^-$ branching ratio integrated in the low-s region.

ACKNOWLEDGMENTS

The authors would like to thank K. Hikasa for carefully reading the manuscript and giving useful comments and S. Uno for discussion on the possibility of the experimental measurement on the lepton invariant mass spectrum near the resonance regions. The works of T.G., Y.O., and M.T. were supported in part by the Grant-in-Aid for Scientific Research from the Ministry of Education, Science and Culture of Japan.

APPENDIX A: ONE-LOOP CORRECTION TO THE HIGGS POTENTIAL

The explicit form of $V_{\rm loop}$ in Eq. (2.5) is given by

$$
\begin{aligned}
V_{\rm loop}=&\frac{3}{32\pi^2}\left[m_{\tilde{t}_1}^4\left(\ln\frac{m_{\tilde{t}_1}^2}{Q^2}-\frac{3}{2}\right)+m_{\tilde{t}_2}^4\left(\ln\frac{m_{\tilde{t}_2}^2}{Q^2}-\frac{3}{2}\right)-2m_t^4\left(\ln\frac{m_t^2}{Q^2}-\frac{3}{2}\right)\right]\\
&+\frac{3}{32\pi^2}\left[m_{\tilde{b}_1}^4\left(\ln\frac{m_{\tilde{b}_1}^2}{Q^2}-\frac{3}{2}\right)+m_{\tilde{b}_2}^4\left(\ln\frac{m_{\tilde{b}_2}^2}{Q^2}-\frac{3}{2}\right)-2m_b^4\left(\ln\frac{m_b^2}{Q^2}-\frac{3}{2}\right)\right]\\
&+\frac{1}{32\pi^2}\left[m_{\tilde{\tau}_1}^4\left(\ln\frac{m_{\tilde{\tau}_1}^2}{Q^2}-\frac{3}{2}\right)+m_{\tilde{\tau}_2}^2\left(\ln\frac{m_{\tilde{\tau}_2}^2}{Q^2}-\frac{3}{2}\right)-2m_\tau^4\left(\ln\frac{m_\tau^2}{Q^2}-\frac{3}{2}\right)\right],
\end{aligned}
\tag{A1}
$$

where Q denotes the renormalization point. The field-dependent masses are given by

$$m_t = f_{U33} h_2^0, \quad m_b = f_{D33} h_1^0, \quad m_\tau = f_{E33} h_1^0, \tag{A2}$$

$$m^2_{\tilde{t}_{1(2)}} = \frac{1}{2}\left[2m_t^2 + m_{Q33}^2 + m_{U33}^2 \mp \sqrt{(m_{Q33}^2 - m_{U33}^2)^2 + 4(-\mu f_{U33} h_1^0 + A_{U33} h_2^0)^2}\right], \tag{A3}$$

$$m^2_{\tilde{b}_{1(2)}} = \frac{1}{2}\left[2m_b^2 + m_{Q33}^2 + m_{D33}^2 \mp \sqrt{(m_{Q33}^2 - m_{D33}^2)^2 + 4(-\mu f_{D33} h_2^0 + A_{D33} h_1^0)^2}\right], \tag{A4}$$

$$m^2_{\tilde{\tau}_{1(2)}} = \frac{1}{2}\left[2m_\tau^2 + m_{L33}^2 + m_{E33}^2 \mp \sqrt{(m_{L33}^2 - m_{E33}^2)^2 + 4(-\mu f_{E33} h_2^0 + A_{E33} h_1^0)^2}\right]. \tag{A5}$$

For simplicity we neglected D-term contributions to the scalar masses.

The radiative electroweak symmetry-breaking condition is

$$\left\langle \frac{\partial V}{\partial h_1^0} \right\rangle = \left\langle \frac{\partial V}{\partial h_2^0} \right\rangle = 0, \tag{A6}$$

where the bracket denotes the value at $h_1^0 = v\cos\beta$ and $h_2^0 = v\sin\beta$. We obtain the following equations for the SUSY Higgs boson mass parameter μ and the soft SUSY-breaking parameter B from Eq. (A6) with the explicit form of the Higgs potential (2.5) and Eq. (A2):

$$\begin{aligned} v^2 = \frac{4}{(g^2+g'^2)(\tan^2\beta - 1)} \Bigg(& (\mu^2 + \Delta_1^2) - (\mu^2 + \Delta_2^2)\tan^2\beta - \frac{3 f_{U33}^2}{16\pi^2}\{[f(m^2_{\tilde{t}_1}) + f(m^2_{\tilde{t}_2}) - 2 f(m_t^2)]\tan^2\beta \\ & + (A_{U33}^2 \tan^2\beta - \mu^2) h(m^2_{\tilde{t}_1}, m^2_{\tilde{t}_2})\} + \frac{3 f_{D33}^2}{16\pi^2}\{[f(m^2_{\tilde{b}_1}) + f(m^2_{\tilde{b}_2}) - 2 f(m_b^2)] + (A_{D33}^2 - \mu^2\tan^2\beta) h(m^2_{\tilde{b}_1}, m^2_{\tilde{b}_2})\} \\ & + \frac{f_{E33}^2}{16\pi^2}\{[f(m^2_{\tilde{\tau}_1}) + f(m^2_{\tilde{\tau}_2}) - 2 f(m_\tau^2)] + (A_{E33}^2 - \mu^2\tan^2\beta) h(m^2_{\tilde{\tau}_1}, m^2_{\tilde{\tau}_2})\} \Bigg), \end{aligned} \tag{A7}$$

$$\begin{aligned} \frac{-B\mu}{\sin\beta\cos\beta} = & (\Delta_1^2 + \Delta_2^2 + 2\mu^2) + \frac{3 f_{U33}^2}{16\pi^2}\{[f(m^2_{\tilde{t}_1}) + f(m^2_{\tilde{t}_2}) - 2 f(m_t^2)] + (A_{U33} - \mu\cot\beta)(A_{U33} - \mu\tan\beta) h(m^2_{\tilde{t}_1}, m^2_{\tilde{t}_2})\} \\ & + \frac{3 f_{D33}^2}{16\pi^2}\{[f(m^2_{\tilde{b}_1}) + f(m^2_{\tilde{b}_2}) - 2 f(m_b^2)] + (A_{D33} - \mu\cot\beta)(A_{D33} - \mu\tan\beta) h(m^2_{\tilde{b}_1}, m^2_{\tilde{b}_2})\} \\ & + \frac{f_{E33}^2}{16\pi^2}\{[f(m^2_{\tilde{\tau}_1}) + f(m^2_{\tilde{\tau}_2}) - 2 f(m_\tau^2)] + (A_{E33} - \mu\cot\beta)(A_{E33} - \mu\tan\beta) h(m^2_{\tilde{\tau}_1}, m^2_{\tilde{\tau}_2})\}, \end{aligned} \tag{A8}$$

where $f(m^2) = m^2[\ln(m^2/Q^2) - 1]$ and $h(m_1^2, m_2^2) = [f(m_1^2) - f(m_2^2)]/[m_1^2 - m_2^2]$.

APPENDIX B: THE EFFECTIVE HAMILTONIAN FOR $b\to s\bar{l}l$

The effective Hamiltonian for the $b\to s\bar{l}l$ is given by

$$H_{\rm eff} = \frac{4G_F}{\sqrt{2}} \sum_{i=1}^{11} C_i(Q) O_i(Q), \tag{B1}$$

in which the operator basis is chosen to be

$$O_1 = (\bar{s}_{L\alpha}\gamma_\mu b_{L\alpha})(\bar{c}_{L\beta}\gamma^\mu c_{L\beta}), \tag{B2}$$

$$O_2 = (\bar{s}_{L\alpha}\gamma_\mu b_{L\beta})(\bar{c}_{L\beta}\gamma^\mu c_{L\alpha}), \tag{B3}$$

$$O_3 = (\bar{s}_{L\alpha}\gamma_\mu b_{L\alpha}) \sum_{q=u,d,s,c,b} (\bar{q}_{L\beta}\gamma^\mu q_{L\beta}), \tag{B4}$$

$$O_4 = (\bar{s}_{L\alpha}\gamma_\mu b_{L\beta}) \sum_{q=u,d,s,c,b} (\bar{q}_{L\beta}\gamma^\mu q_{L\alpha}), \tag{B5}$$

$$O_5 = (\bar{s}_{L\alpha}\gamma_\mu b_{L\alpha}) \sum_{q=u,d,s,c,b} (\bar{q}_{R\beta}\gamma^\mu q_{R\beta}), \tag{B6}$$

$$O_6 = (\bar{s}_{L\alpha}\gamma_\mu b_{L\beta}) \sum_{q=u,d,s,c,b} (\bar{q}_{R\beta}\gamma^\mu q_{R\alpha}), \tag{B7}$$

$$O_7 = \frac{e}{16\pi^2} m_b (\bar{s}_{L\alpha}\sigma_{\mu\nu} b_{R\alpha}) F^{\mu\nu}, \tag{B8}$$

$$O_8=\frac{g_s}{16\pi^2}\, m_b(\overline{s_{L\alpha}}T^a_{\alpha\beta}\sigma_{\mu\nu}b_{R\alpha})G^{a\mu\nu}, \tag{B9}$$

$$O_9=\frac{e^2}{16\pi^2}\,(\overline{s_{L\alpha}}\gamma_\mu b_{L\alpha})(\overline{l\gamma}^\mu l), \tag{B10}$$

$$O_{10}=\frac{e^2}{16\pi^2}\,(\overline{s_{L\alpha}}\gamma_\mu b_{L\alpha})(\overline{l\gamma}^\mu\gamma_5 l), \tag{B11}$$

$$O_{11}=\frac{g^2}{16\pi^2}\,(\overline{s_{L\alpha}}\gamma_\mu b_{L\alpha})\sum_{i=e,\mu,\tau}[\overline{\nu_i}\gamma^\mu(1-\gamma_5)\nu_i]. \tag{B12}$$

APPENDIX C: WILSON COEFFICIENTS AT THE ELECTROWEAK SCALE

In this appendix, we give explicit forms of each contribution to Wilson coefficients at the electroweak scale [4,9].

1. $C_7(m_W)$

$$C_7(m_W)=C_7^W+C_7^{H^-}+C_7^{\tilde\chi^-}+C_7^{\tilde G}+C_7^{\tilde\chi^0}, \tag{C1}$$

$$C_7^W=\frac{3}{2}\,\lambda_t x_{tW}\left[\frac{2}{3}\,f_1(x_{tW})+f_2(x_{tW})\right], \tag{C2}$$

$$C_7^{H^-}=\frac{1}{2}\,\lambda_t x_{th}\left[\cot^2\beta\left\{\frac{2}{3}\,f_1(x_{th})+f_2(x_{th})\right\}+\left\{\frac{2}{3}\,f_3(x_{th})+f_4(x_{th})\right\}\right], \tag{C3}$$

$$C_7^{\tilde\chi^-}=-\sum_{\alpha=1}^{2}\sum_{I=1}^{6}x_{W\tilde u_I}(\Gamma^{d\dagger}_{CL})^I_{\alpha 2}\times\left[(\Gamma^d_{CL})_I^{\alpha 3}\left\{f_1(x_{\tilde\chi^-_\alpha\tilde u_I})+\frac{2}{3}\,f_2(x_{\tilde\chi^-_\alpha\tilde u_I})\right\}+(\Gamma^d_{CR})_I^{\alpha 3}\,\frac{m_{\tilde\chi^-_\alpha}}{m_b}\left\{f_3(x_{\tilde\chi^-_\alpha\tilde u_I})+\frac{2}{3}\,f_4(x_{\tilde\chi^-_\alpha\tilde u_I})\right\}\right], \tag{C4}$$

$$C_7^{\tilde G}=\frac{8}{9}\,\frac{g_s^2}{g^2}\sum_{I=1}^{6}x_{W\tilde d_I}(\Gamma^{d\dagger}_{GL})^I_2\times\left[(\Gamma^d_{GL})_I^3 f_2(x_{\tilde G\tilde d_I})+(\Gamma^d_{GR})_I^3\,\frac{m_{\tilde G}}{m_b}\,f_4(x_{\tilde G\tilde d_I})\right], \tag{C5}$$

$$C_7^{\tilde\chi^0}=\frac{1}{3}\sum_{\alpha=1}^{4}\sum_{I=1}^{6}x_{W\tilde d_I}(\Gamma^{d\dagger}_{NL})^I_{\alpha 2}\times\left[(\Gamma^d_{NL})_I^{\alpha 3}f_2(x_{\tilde\chi^0_\alpha\tilde u_I})+(\Gamma^d_{NR})_I^{\alpha 3}\,\frac{m_{\tilde\chi^0_\alpha}}{m_b}\,f_4(x_{\tilde\chi^0_\alpha\tilde u_I})\right], \tag{C6}$$

where $x_{ij}=m_i^2/m_j^2$ and m_i is the mass of the particle i. $f_i(x)$ are the one-loop functions, which are given in Appendix E. The matrix $\Gamma^d_{CL(R)}$ represents the coupling constant of chargino–(up-type-)squark–(down-type-)quark, $\Gamma^d_{NL(R)}$ represents that of neutralino–(down-type-)squark–(down-type-)quark and $\Gamma^d_{GL(R)}$ represents that of gluino–(down-type-)squark–(down-type-)quark, which are found in Appendix D.

2. $C_8(m_W)$

$$C_8(m_W)=C_8^W+C_8^{H^-}+C_8^{\tilde\chi^-}+C_8^{\tilde G}+C_8^{\tilde\chi^0}, \tag{C7}$$

$$C_8^W=\frac{3}{2}\,\lambda_t x_{tW}f_1(x_{tW}), \tag{C8}$$

$$C_8^{H^-}=\frac{1}{2}\,\lambda_t x_{th}[\cot^2\beta f_1(x_{th})+f_3(x_{th})], \tag{C9}$$

$$C_8^{\tilde\chi^-}=-\sum_{\alpha=1}^{2}\sum_{I=1}^{6}x_{W\tilde u_I}(\Gamma^{d\dagger}_{CL})^I_{\alpha 2}\left[(\Gamma^d_{CL})_I^{\alpha 3}f_2(x_{\tilde\chi^-_\alpha\tilde u_I})+(\Gamma^d_{CR})_I^{\alpha 3}\,\frac{m_{\tilde\chi^-_\alpha}}{m_b}\,f_4(x_{\tilde\chi^-_\alpha\tilde u_I})\right], \tag{C10}$$

$$C_8^{\tilde G}=\frac{g_s^2}{g^2}\sum_{I=1}^{6}x_{W\tilde d_I}(\Gamma^{d\dagger}_{GL})^I_2\left[(\Gamma^d_{GL})_I^3\left\{3f_1(x_{\tilde G\tilde d_I})+\frac{1}{3}\,f_2(x_{\tilde G\tilde d_I})\right\}+(\Gamma^d_{GR})_I^3\,\frac{m_{\tilde G}}{m_b}\left\{3f_3(x_{\tilde G\tilde d_I})+\frac{1}{3}\,f_4(x_{\tilde G\tilde d_I})\right\}\right], \tag{C11}$$

$$C_8^{\tilde\chi^0}=-\sum_{\alpha=1}^{4}\sum_{I=1}^{6}x_{W\tilde d_I}(\Gamma^{d\dagger}_{NL})^I_{\alpha 2}\left[(\Gamma^d_{NL})_I^{\alpha 3}f_2(x_{\tilde\chi^0_\alpha\tilde d_I})+(\Gamma^d_{NR})_I^{\alpha 3}\,\frac{m_{\tilde\chi^0_\alpha}}{m_b}\,f_4(x_{\tilde\chi^0_\alpha\tilde d_I})\right]. \tag{C12}$$

3. $C_9(m_W)$

$$C_9(m_W)=C_{9,\gamma}+C_{9,Z}+C_{9,\mathrm{box}}, \tag{C13}$$

$$C_{9,\gamma}=C_{9,\gamma}^W+C_{9,\gamma}^{H^-}+C_{9,\gamma}^{\tilde\chi^-}+C_{9,\gamma}^{\tilde G}+C_{9,\gamma}^{\tilde\chi^0}, \tag{C14}$$

$$C_{9,Z}=C_{9,Z}^W+C_{9,Z}^{H^-}+C_{9,Z}^{\tilde\chi^-}+C_{9,Z}^{\tilde G}+C_{9,Z}^{\tilde\chi^0}, \tag{C15}$$

$$C_{9,\mathrm{box}}=C_{9,\mathrm{box}}^W+C_{9,\mathrm{box}}^{\tilde\chi^-}+C_{9,\mathrm{box}}^{\tilde\chi^0}, \tag{C16}$$

$$C_{9,\gamma}^W=\lambda_t\left[x_{tW}\left\{\frac{2}{3}\,f_7(x_{tW})+f_8(x_{tW})\right\}+\frac{4}{9}\left(\frac{\ln x_{tW}}{x_{tW}-1}-1\right)\right], \tag{C17}$$

$$C_{9,\gamma}^{H^-}=\lambda_t\cot^2\beta x_{th}\left[\frac{2}{3}\,f_5(x_{th})-f_6(x_{th})\right], \tag{C18}$$

$$C_{9,\gamma}^{\tilde{\chi}^-}=2\sum_{\alpha=1}^{2}\sum_{I=1}^{6}x_{W\tilde{u}_I}(\Gamma_{CL}^{d})_I^{\alpha 3}(\Gamma_{CL}^{d\dagger})_{\alpha 2}^{I}\left[\frac{2}{3}f_6(x_{\tilde{\chi}_\alpha^-\tilde{u}_I})-f_5(x_{\tilde{\chi}_\alpha^-\tilde{u}_I})\right],\tag{C19}$$

$$C_{9,\gamma}^{\tilde{G}}=-\frac{16}{9}\frac{g_s^2}{g^2}\sum_{I=1}^{6}x_{W\tilde{d}_I}(\Gamma_{GL}^{d})_I^{3}(\Gamma_{GL}^{d\dagger})_2^{I}f_6(x_{\tilde{G}\tilde{d}_I}),\tag{C20}$$

$$C_{9,\gamma}^{\tilde{\chi}^0}=-\frac{2}{3}\sum_{\alpha=1}^{4}\sum_{I=1}^{6}x_{W\tilde{d}_I}(\Gamma_{NL}^{d})_I^{\alpha 3}(\Gamma_{NL}^{d\dagger})_{\alpha 2}^{I}f_6(x_{\tilde{\chi}_\alpha^0\tilde{d}_I}),\tag{C21}$$

$$C_{9,Z}^{W}=\left(-1+\frac{1}{4\sin^2\theta_W}\right)x_{tW}f_9(x_{tW}),\tag{C22}$$

$$C_{9,Z}^{H^-}=\frac{1}{2}\left(-1+\frac{1}{4\sin^2\theta_W}\right)\cot^2\beta x_{tW}x_{th}[f_3(x_{th})+f_4(x_{th})],\tag{C23}$$

$$C_{9,Z}^{\tilde{\chi}^-}=2\left(-1+\frac{1}{4\sin^2\theta_W}\right)\sum_{\alpha,\beta=1}^{2}\sum_{I,J=1}^{6}(\Gamma_{CL}^{d})_I^{\alpha 3}(\Gamma_{CL}^{d\dagger})_{\beta 2}^{J}\times\Bigg[\delta_{\alpha\beta}g_2(x_{\tilde{u}_J\tilde{\chi}_\beta^-},x_{\tilde{u}_I\tilde{\chi}_\alpha^-})\sum_{M=1}^{3}(\tilde{U}_U)_J^M(\tilde{U}_U^\dagger)_M^I+\delta_{IJ}\{2\sqrt{x_{\tilde{\chi}_\alpha^-\tilde{u}_I}x_{\tilde{\chi}_\beta^-\tilde{u}_J}}g_1(x_{\tilde{\chi}_\alpha^-\tilde{u}_I},x_{\tilde{\chi}_\beta^-\tilde{u}_J})(U_-^\dagger)_\alpha^1(U_-)_1^\beta+\ln x_{W\tilde{u}_I}-g_2(x_{\tilde{\chi}_\alpha^-\tilde{u}_I},x_{\tilde{\chi}_\beta^-\tilde{u}_J})(U_+^\dagger)_\alpha^1(U_+)_1^\beta\}\Bigg],\tag{C24}$$

$$C_{9,Z}^{\tilde{G}}=-\frac{g_s^2}{g^2}\left(-1+\frac{1}{4\sin^2\theta_W}\right)\frac{4}{3}\sum_{I,J=1}^{6}\sum_{M=1}^{3}(\Gamma_{GL}^{d})_I^{6}(\Gamma_{GL}^{d\dagger})_5^{J}\times(\Gamma_{GR}^{d})_J^M(\Gamma_{GR}^{d\dagger})_M^I g_2(x_{\tilde{d}_I\tilde{G}},x_{\tilde{d}_J\tilde{G}}),\tag{C25}$$

$$C_{9,Z}^{\tilde{\chi}^0}=\frac{1}{2}\left(-1+\frac{1}{4\sin^2\theta_W}\right)\sum_{\alpha,\beta=1}^{4}\sum_{I,J=1}^{6}(\Gamma_{NL}^{d})_I^{\alpha 3}(\Gamma_{NL}^{d\dagger})_{\beta 2}^{J}\times\Bigg[\delta_{\alpha\beta}g_2(x_{\tilde{d}_J\tilde{\chi}_\beta^0},x_{\tilde{d}_I\tilde{\chi}_\alpha^0})\sum_{M=1}^{3}(\tilde{U}_D)_J^M(\tilde{U}_D^\dagger)_M^I+\delta_{IJ}\{-2\sqrt{x_{\tilde{\chi}_\beta^0\tilde{d}_I}x_{\tilde{\chi}_\alpha^0\tilde{d}_I}}g_1(x_{\tilde{\chi}_\beta^0\tilde{d}_I},x_{\tilde{\chi}_\alpha^0\tilde{d}_I})G_{\beta\alpha}+\ln x_{W\tilde{d}_I}-g_2(x_{\tilde{\chi}_\beta^0\tilde{d}_I},x_{\tilde{\chi}_\alpha^0\tilde{d}_I})G_{\alpha\beta}\}\Bigg],\tag{C26}$$

$$C_{9,\mathrm{box}}^{W}=\lambda_t\frac{1}{4\sin^2\theta_W}[g_3(x_{tW},0)-g_3(0,0)],\tag{C27}$$

$$C_{9,\mathrm{box}}^{\tilde{\chi}^-}=\frac{1}{4\sin^2\theta_W}\sum_{\alpha,\beta=1}^{2}\sum_{I=1}^{6}\sum_{J=1}^{3}x_{W\tilde{\chi}_\alpha^-}(\Gamma_{CL}^{d})_I^{\alpha 3}(\Gamma_{CL}^{d\dagger})_{\beta 2}^{I}\times(\Gamma_{CL}^{l})_J^{\beta i}(\Gamma_{CL}^{l\dagger})_{\alpha i}^{J}g_6(x_{\tilde{u}_I\tilde{\chi}_\alpha^-},x_{\tilde{\nu}_J\tilde{\chi}_\alpha^-},x_{\tilde{\chi}_\beta^-\tilde{\chi}_\alpha^-}),\tag{C28}$$

$$C_{9,\mathrm{box}}^{\tilde{\chi}^0}=\frac{1}{4\sin^2\theta_W}\sum_{\alpha,\beta=1}^{4}\sum_{I,J=1}^{6}x_{W\tilde{\chi}_\alpha^0}(\Gamma_{NL}^{d})_I^{\alpha 3}(\Gamma_{NL}^{d\dagger})_{\beta 2}^{I}\times[\{(\Gamma_{NL}^{l})_J^{\beta i}(\Gamma_{NL}^{l\dagger})_{\alpha i}^{J}-(\Gamma_{NR}^{l})_J^{\alpha i}(\Gamma_{NR}^{l\dagger})_{\beta i}^{J}\}\times g_6(x_{\tilde{d}_J\tilde{\chi}_\alpha^0},x_{\tilde{l}_I\tilde{\chi}_\alpha^0},x_{\tilde{\chi}_\beta^0\tilde{\chi}_\alpha^0})-\{(\Gamma_{NL}^{l})_J^{\beta i}(\Gamma_{NL}^{l\dagger})_{\alpha i}^{J}-(\Gamma_{NR}^{l})_J^{\alpha i}(\Gamma_{NR}^{l\dagger})_{\beta i}^{J}\}\times 2\sqrt{x_{\tilde{\chi}_\beta^0\tilde{\chi}_\alpha^0}}g_5(x_{\tilde{d}_J\tilde{\chi}_\alpha^0},x_{\tilde{l}_I\tilde{\chi}_\alpha^0},x_{\tilde{\chi}_\alpha^0\tilde{\chi}_\alpha^0})].\tag{C29}$$

The matrix $\Gamma_{CL(R)}^{l}$ represents the coupling constant of chargino-sneutrino-lepton and $\Gamma_{NL(R)}^{l}$ that of neutralino-slepton-lepton, which are found in Appendix D. Note that index i represents the generation of the final lepton and is not summed here.

4. $C_{10}(m_W)$

$$C_{10}(m_W)=C_{10,Z}+C_{10,\mathrm{box}},\tag{C30}$$

$$C_{10,Z}=C_{10,Z}^{W}+C_{10,Z}^{H^-}+C_{10,Z}^{\tilde{\chi}^-}+C_{10,Z}^{\tilde{G}}+C_{10,Z}^{\tilde{\chi}^0},\tag{C31}$$

$$C_{10,\mathrm{box}}=C_{10,\mathrm{box}}^{W}+C_{10,\mathrm{box}}^{\tilde{\chi}^-}+C_{10,\mathrm{box}}^{\tilde{\chi}^0},\tag{C32}$$

$$C_{10,Z}^{i}=\frac{-1/(4\sin^2\theta_W)}{-1+1/(4\sin^2\theta_W)}C_{9,Z}^{i},\quad i=W,H^-,\tilde{\chi}^-,\tilde{G},\tilde{\chi}^0,\tag{C33}$$

$$C_{10,\mathrm{box}}^{i}=-C_{9,\mathrm{box}}^{i},\quad i=W,\tilde{\chi}^-,\tag{C34}$$

$$C_{10,\mathrm{box}}^{\tilde{\chi}^0}=\frac{1}{4\sin^2\theta_W}\sum_{\alpha,\beta=1}^{4}\sum_{I,J=1}^{6}x_{W\tilde{\chi}_\alpha^0}(\Gamma_{NL}^{d})_I^{\alpha 3}(\Gamma_{NL}^{d\dagger})_{\beta 2}^{I}\times[-\{(\Gamma_{NL}^{l})_J^{\beta i}(\Gamma_{NL}^{l\dagger})_{\alpha i}^{J}+(\Gamma_{NR}^{l})_J^{\alpha i}(\Gamma_{NR}^{l\dagger})_{\beta i}^{J}\}\times g_6(x_{\tilde{d}_J\tilde{\chi}_\alpha^0},x_{\tilde{l}_I\tilde{\chi}_\alpha^0},x_{\tilde{\chi}_\beta^0\tilde{\chi}_\alpha^0})+\{(\Gamma_{NL}^{l})_J^{\beta i}(\Gamma_{NL}^{l\dagger})_{\alpha i}^{J}+(\Gamma_{NR}^{l})_J^{\alpha i}(\Gamma_{NR}^{l\dagger})_{\beta i}^{J}\}\times 2\sqrt{x_{\tilde{\chi}_\beta^0\tilde{\chi}_\alpha^0}}g_5(x_{\tilde{d}_J\tilde{\chi}_\alpha^0},x_{\tilde{l}_I\tilde{\chi}_\alpha^0},x_{\tilde{\chi}_\beta^0\tilde{\chi}_\alpha^0})].\tag{C35}$$

5. $C_{11}(m_W)$

$$C_{11}(m_W)=C_{11,Z}+C_{11,\mathrm{box}}\tag{C36}$$

$$C_{11,Z}=C_{11,Z}^{W}+C_{11,Z}^{H^-}+C_{11,Z}^{\tilde{\chi}^-}+C_{11,Z}^{\tilde{G}}+C_{11,Z}^{\tilde{\chi}^0},\tag{C37}$$

$$C_{11,\mathrm{box}}=C_{11,\mathrm{box}}^{W}+C_{11,\mathrm{box}}^{\tilde{\chi}^-}+C_{11,\mathrm{box}}^{\tilde{\chi}^0},\tag{C38}$$

$$C_{11,Z}^{i}=\sin\theta_W^2C_{10,Z},\quad i=W,H^-,\tilde{\chi}^-,\tilde{G},\tilde{\chi}^0,\tag{C39}$$

$$C_{11,\mathrm{box}}^{W}=4\sin\theta_W^2C_{10,\mathrm{box}}^{W},\tag{C40}$$

$$C^{\tilde{\chi}^-}_{11,\mathrm{box}} = -\frac{1}{4}\sum_{\alpha,\beta=1}^{2}\sum_{I,J=1}^{6} x_{W\tilde{\chi}^-_\alpha}(\Gamma^d_{CL})^{\alpha 3}_I(\Gamma^{d\dagger}_{CL})^I_{\beta 2} \times(\Gamma^\nu_{CL})^{\alpha i}_J(\Gamma^{\nu\dagger}_{CL})^J_{\beta i} \times 2\sqrt{x_{\tilde{\chi}^-_\beta\tilde{\chi}^-_\alpha}}\,g_5(x_{\tilde{u}_I\tilde{\chi}^-_\alpha},x_{\tilde{l}_J\tilde{\chi}^-_\alpha},x_{\tilde{\chi}^-_\beta\tilde{\chi}^-_\alpha}), \tag{C41}$$

$$C^{\tilde{\chi}^0}_{11,\mathrm{box}} = \frac{1}{4}\sum_{\alpha,\beta=1}^{4}\sum_{I=1}^{6}\sum_{J=1}^{3} x_{W\tilde{\chi}^0_\alpha}(\Gamma^d_{NL})^{\alpha 3}_I(\Gamma^{d\dagger}_{NL})^I_{\beta 2}[-(\Gamma^\nu_{NL})^{\alpha i}_J \times(\Gamma^{\nu\dagger}_{NL})^J_{\beta i}2\sqrt{x_{\tilde{\chi}^0_\beta\tilde{\chi}^0_\alpha}}\,g_5(x_{\tilde{\nu}_J\tilde{\chi}^0_\alpha},x_{\tilde{d}_I\tilde{\chi}^0_\alpha},x_{\tilde{\chi}^0_\beta\tilde{\chi}^0_\alpha}) +(\Gamma^\nu_{NL})^{\beta i}_J(\Gamma^{\nu\dagger}_{NL})^J_{\alpha i}g_6(x_{\tilde{\nu}_J\tilde{\chi}^0_\alpha},x_{\tilde{d}_I\tilde{\chi}^0_\alpha},x_{\tilde{\chi}^0_\beta\tilde{\chi}^0_\alpha})]. \tag{C42}$$

APPENDIX D: FEYNMAN RULES

In this appendix, we give our notations. The mass matrix of chargino is given by

$$\mathcal{L} = -(\tilde{W}^-\tilde{h}_1^-)\begin{pmatrix} M_2 & \sqrt{2}m_W\sin\beta \\ \sqrt{2}m_W\cos\beta & \mu \end{pmatrix}\begin{pmatrix}\tilde{W}^+\\ \tilde{h}_2^+\end{pmatrix}+\mathrm{H.c.} \tag{D1}$$

Diagonalizing this mass matrix, mass eigenstates of chargino χ_i $(i=1,2)$ are given by

$$\begin{pmatrix}\tilde{\chi}^+_1\\ \tilde{\chi}^+_2\end{pmatrix} = U_+\begin{pmatrix}\tilde{W}^+\\ \tilde{h}_2^+\end{pmatrix},\quad \begin{pmatrix}\tilde{\chi}^-_1\\ \tilde{\chi}^-_2\end{pmatrix} = U_-\begin{pmatrix}\tilde{W}^-\\ \tilde{h}_1^-\end{pmatrix}. \tag{D2}$$

The mass matrix of the neutralino is given by

$$\mathcal{L} = -\frac{1}{2}(\tilde{B}\ \tilde{W}^3\ \tilde{h}_1^0\ \tilde{h}_2^0) \times\begin{pmatrix} M_1 & 0 & -m_Z s_W c_\beta & m_Z s_W s_\beta \\ 0 & M_2 & m_Z c_W c_\beta & -m_Z c_W s_\beta \\ -m_Z s_W c_\beta & m_Z c_W c_\beta & 0 & -\mu \\ m_Z s_W s_\beta & -m_Z c_W s_\beta & -\mu & 0 \end{pmatrix} \times\begin{pmatrix}\tilde{B}\\ \tilde{W}^3\\ \tilde{h}_1^0\\ \tilde{h}_2^0\end{pmatrix}, \tag{D3}$$

where $s_W=\sin\theta_W$, $c_W=\cos\theta_W$, $s_\beta=\sin\beta$, and $c_\beta=\cos\beta$. Diagonalizing this mass matrix, mass eigenstates of neutralino are given by

$$\begin{pmatrix}\tilde{\chi}^1_0\\ \tilde{\chi}^2_0\\ \tilde{\chi}^3_0\\ \tilde{\chi}^4_0\end{pmatrix} = U_N\begin{pmatrix}\tilde{B}\\ \tilde{W}^3\\ \tilde{h}_1^0\\ \tilde{h}_2^0\end{pmatrix}. \tag{D4}$$

The relevant interaction Lagrangian for the $b\to s l\bar{l}$ process is written as follows.

Chargino-quark(lepton)-squark(slepton) interaction

$$\mathcal{L} = -g\overline{\tilde{\chi}^-_\alpha}[(\Gamma^d_{CL})^{\alpha j}_I P_L+(\Gamma^d_{CR})^{\alpha j}_I P_R]d_j\tilde{u}^*_I -g\overline{\tilde{\chi}^-_\alpha}[(\Gamma^l_{CL})^{\alpha j}_I P_L+(\Gamma^l_{CR})^{\alpha j}_I P_R]l_j\tilde{\nu}^*_I -g\overline{(\tilde{\chi}^-)^C_\alpha}(\Gamma^\nu_{CL})^{\alpha j}_I P_L\nu_j\tilde{l}^*_I+\mathrm{H.c.},$$

$$P_{R(L)} = \frac{1}{2}(1\pm\gamma_5). \tag{D5}$$

The mixing matrices $\Gamma^d_{CL(R)}$, $\Gamma^l_{CL(R)}$, and Γ^ν_{CL} are given by

$$(\Gamma^d_{CL})^{\alpha j}_I = (\tilde{U}_U)^j_I(U_+)^{*\alpha}_1-(\tilde{U}_U)^{k+3}_I \times\frac{m^{(u)}_k}{\sqrt{2}m_W\sin\beta}(U_+)^{*\alpha}_2V_{kj}, \tag{D6}$$

$$(\Gamma^d_{CR})^{\alpha j}_I = (\tilde{U}_U)^k_I\frac{m^{(d)}_k}{\sqrt{2}m_W\cos\beta}(U_-)^\alpha_2, \tag{D7}$$

$$(\Gamma^l_{CL})^{\alpha j}_I = (\tilde{U}_\nu)^j_I(U_+)^{*\alpha}_1, \tag{D8}$$

$$(\Gamma^\nu_{CL})^{\alpha j}_I = (\tilde{U}_l)^j_I(U_-)^\alpha_1, \tag{D9}$$

where the matrices $\tilde{U}_U$, $\tilde{U}_l$, and $\tilde{U}_\nu$ are the unitary matrices which diagonalize the up-type squark mass matrix, the slepton mass matrix, and the sneutrino mass matrix, respectively. V is the CKM matrix. Note that we neglect the small contribution proportional to the Yukawa couplings of the lepton.

Neutralino-quark(lepton)-squark(slepton) interaction

$$\mathcal{L} = -g\overline{\tilde{\chi}^0_\alpha}[(\Gamma^d_{NL})^{\alpha j}_I P_L+(\Gamma^d_{NR})^{\alpha j}_I P_R]d_j\tilde{d}^*_I -g\overline{\tilde{\chi}^0_\alpha}[(\Gamma^l_{NL})^{\alpha j}_I P_L+(\Gamma^l_{NR})^{\alpha j}_I P_R]l_j\tilde{l}^*_I -g\overline{\tilde{\chi}^0_\alpha}(\Gamma^\nu_{NL})^{\alpha j}_I P_L\nu_j\tilde{\nu}^*_I+\mathrm{H.c.} \tag{D10}$$

The mixing matrices $\Gamma^d_{NL(R)}$, $\Gamma^l_{NL(R)}$, and Γ^ν_{NL} are given by

$$(\Gamma^d_{NL})^{\alpha j}_I = \sqrt{2}\left[\frac{1}{2}(U_N)^\alpha_2-\frac{1}{6}\tan\theta_W(U_N)^\alpha_1\right](\tilde{U}_D)^j_I -\frac{m^d_j}{\sqrt{2}m_W\cos\beta}(U_N)^\alpha_3(\tilde{U}_D)^{j+3}_I, \tag{D11}$$

$$(\Gamma^d_{NR})^{\alpha j}_I = \sqrt{2}\left[-\frac{1}{3}\tan\theta_W(U^\dagger_N)^\alpha_1\right](\tilde{U}_D)^{j+3}_I -\frac{m^d_j}{\sqrt{2}m_W\cos\beta}(U^\dagger_N)^\alpha_3(\tilde{U}_D)^j_I, \tag{D12}$$

$$(\Gamma^l_{NL})^{\alpha j}_I = \sqrt{2}\left[\frac{1}{2}(U_N)^\alpha_2+\frac{1}{2}\tan\theta_W(U_N)^\alpha_1\right](\tilde{U}^\dagger_L)^i_I, \tag{D13}$$

$$(\Gamma^l_{NR})^{\alpha j}_I = \sqrt{2}[-\tan\theta_W(U^\dagger_N)^\alpha_1](\tilde{U}^\dagger_l)^{j+3}_I, \tag{D14}$$

$$G_{\alpha\beta} = (U^\dagger_N)^3_\alpha(U_N)^\beta_3-(U^\dagger_N)^4_\alpha(U_N)^\beta_4, \tag{D15}$$

$$(\Gamma^{\nu}_{NL})^{\alpha j}_{I}=\sqrt{2}\left[-\frac{1}{2}(U_N)^{\alpha}_{2}+\frac{1}{2}\tan\theta_W(U_N)^{\alpha}_{1}\right](\widetilde{U}^{\dagger}_{\nu})^{j}_{I}, \tag{D16}$$

where the matrix $\widetilde{U}_D$ is the unitary matrix which diagonalizes the down-type squark mass matrix.

Gluino-quark-squark interaction

$$\mathcal{L}=-g_s\sqrt{2}(T^a)_{\alpha\beta}\overline{\widetilde{G}^a}[(\Gamma^{d}_{GL})^{j}_{I}P_L+(\Gamma^{d}_{GR})^{j}_{I}P_R]d_{j\alpha}\widetilde{d}^{*}_{I\beta}, \tag{D17}$$

where the mixing matrices $\Gamma^{d}_{GL(R)}$ are given by

$$(\Gamma^{d}_{GL})^{j}_{I}=(\widetilde{U}_D)^{j}_{I}, \tag{D18}$$

$$(\Gamma^{d}_{GR})^{j}_{I}=-(\widetilde{U}_D)^{j+3}_{I}. \tag{D19}$$

APPENDIX E: ONE-LOOP FUNCTIONS

These are the one-loop functions which appear in calculating the penguin or box diagrams;

$$f_1(x)=\frac{1}{12(x-1)^4}(x^3-6x^2+3x+2+6x\ln x), \tag{E1}$$

$$f_2(x)=\frac{1}{12(x-1)^4}(2x^3+3x^2-6x+1-6x^2\ln x), \tag{E2}$$

$$f_3(x)=\frac{1}{2(x-1)^3}(x^2-4x+3+2\ln x), \tag{E3}$$

$$f_4(x)=\frac{1}{2(x-1)^3}(x^2-1+2x\ln x), \tag{E4}$$

$$f_5(x)=\frac{1}{36(x-1)^4}[7x^3-36x^2+45x-16+(18x-12)\ln x], \tag{E5}$$

$$f_6(x)=\frac{1}{36(x-1)^4}(-11x^3+18x^2-9x+2+6x^3\ln x), \tag{E6}$$

$$f_7(x)=\frac{1}{12(x-1)^4}[x^3+10x^2-29x+18-(8x^2-6x-8)\ln x], \tag{E7}$$

$$f_8(x)=\frac{1}{12(x-1)^4}[-7x^3+8x^2+11x-12-(2x^3-20x^2+24x)\ln x], \tag{E8}$$

$$f_9(x)=\frac{1}{2(x-1)^2}[x^2-7x+6+(3x+2)\ln x], \tag{E9}$$

$$g_1(x,y)=\frac{1}{x-y}\left[\frac{x}{x-1}\ln x-(x\leftrightarrow y)\right], \tag{E10}$$

$$g_2(x,y)=\frac{1}{x-y}\left[\frac{x^2}{x-1}\ln x-\frac{3}{2}x-(x\leftrightarrow y)\right], \tag{E11}$$

$$g_3(x,y)=\frac{1}{x-y}\left[\frac{x^2}{(x-1)^2}\ln x-\frac{1}{x-1}-(x\leftrightarrow y)\right], \tag{E12}$$

$$g_5(x,y,z)=-\frac{1}{x-y}\left[\frac{1}{x-z}\left[\frac{x}{x-1}\ln x-(x\leftrightarrow z)\right]-(x\leftrightarrow y)\right], \tag{E13}$$

$$g_6(x,y,z)=\frac{1}{x-y}\times\left[\frac{1}{x-z}\left[\frac{x^2}{x-1}\ln x-\frac{3x}{2}-(x\leftrightarrow z)\right]-(x\leftrightarrow y)\right]. \tag{E14}$$

APPENDIX F: THE QCD CORRECTION

With $C_i(m_W)$ as the initial condition, we obtain the solution of RGE's in the LLA approximation [8,14]:

$$C_1(Q)=\frac{1}{2}C_2(m_W)(\eta^{6/23}-\eta^{-12/23}), \tag{F1}$$

$$C_2(Q)=\frac{1}{2}C_2(m_W)(\eta^{6/23}+\eta^{-12/23}), \tag{F2}$$

$$C_3(Q)=C_2(m_W)\Big(-0.0112\eta^{-0.8994}+\frac{1}{6}\eta^{-12/23}-0.1403\eta^{-0.4230}+0.0054\eta^{0.1456}-0.0714\eta^{6/23}+0.0509\eta^{0.4086}\Big), \tag{F3}$$

$$C_4(Q)=C_2(m_W)\Big(0.0156\eta^{-0.8994}-\frac{1}{6}\eta^{-12/23}+0.1214\eta^{-0.4230}+0.0026\eta^{0.1456}-0.0714\eta^{6/23}+0.0984\eta^{0.4086}\Big), \tag{F4}$$

$$C_5(Q)=C_2(m_W)(-0.0025\eta^{-0.8994}+0.0117\eta^{-0.4230}+0.0304\eta^{0.1456}-0.0397\eta^{0.4086}), \tag{F5}$$

$$C_6(Q)=C_2(m_W)(-0.0462\eta^{-0.8994}+0.0239\eta^{-0.4230}-0.0112\eta^{0.1456}+0.0335\eta^{0.4086}), \tag{F6}$$

$$C_7(Q)=C_7(m_W)\,\eta^{16/23}+C_8(m_W)\,\frac{8}{3}\,(\eta^{14/23}-\eta^{16/23})$$
$$+C_2(m_W)(-0.0185\,\eta^{-0.8994}-0.0714\,\eta^{-12/23}$$
$$-0.0380\,\eta^{-0.4230}-0.0057\,\eta^{0.1456}-0.4286\,\eta^{6/23}$$
$$-0.6494\,\eta^{0.4086}+2.2996\,\eta^{14/23}-1.0880\,\eta^{16/23}), \tag{F7}$$

$$C_8(Q)=C_8(m_W)\,\eta^{14/23}+C_2(m_W)$$
$$\times(-0.0571\,\eta^{-0.8994}+0.0873\,\eta^{-0.4230}$$
$$+0.0209\,\eta^{0.1456}$$
$$-0.9135\,\eta^{0.4086}+0.8623\,\eta^{14/23}), \tag{F8}$$

$$C_9(Q)=C_9(m_W)+\frac{\pi}{\alpha_s(m_W)}\,C_2(m_W)$$
$$\times(-0.1875+0.1648\,\eta^{1-0.8994}+0.2424\,\eta^{1-12/23}$$
$$+0.1384\,\eta^{1-0.4230}-0.0073\,\eta^{1+0.1456}$$
$$-0.3941\,\eta^{1+6/23}+0.0433\,\eta^{1+0.4086}), \tag{F9}$$

$$C_{10}(Q)=C_{10}(m_W),$$
$$C_{11}(Q)=C_{11}(m_W), \tag{F10}$$

where $\eta=\alpha_s(m_W)/\alpha_s(Q)$.

APPENDIX G: THE KINEMATICAL FUNCTIONS

In this appendix we show the explicit form of kinematical functions in Eq. (3.6) and Eq. (3.10). Here $\hat{s}$, $\hat{m}_s$, and $\hat{m}_l$ means s/m_b^2, m_s/m_b, and m_l/m_b:

$$w(\hat{s})=\sqrt{[\hat{s}-(1+\hat{m}_s)^2][\hat{s}-(1-\hat{m}_s)^2]}, \tag{G1}$$

$$\alpha_1(\hat{s},\hat{m}_s,\hat{m}_l)=\left(1+\frac{2\hat{m}_l^2}{\hat{s}}\right)[-2\hat{s}^2+\hat{s}(1+\hat{m}_s^2)+(1-\hat{m}_s^2)^2], \tag{G2}$$

$$\alpha_2(\hat{s},\hat{m}_s,\hat{m}_l)=[-2\hat{s}^2+\hat{s}(1+\hat{m}_s^2)+(1-\hat{m}_s^2)^2]$$
$$+\frac{2\hat{m}_l^2}{\hat{s}}\,[4\hat{s}^2-5(1+\hat{m}_s^2)\hat{s}+(1-\hat{m}_s^2)^2], \tag{G3}$$

$$\alpha_3(\hat{s},\hat{m}_s,\hat{m}_l)=\left(1+\frac{2\hat{m}_l^2}{\hat{s}}\right)[-(1+\hat{m}_s^2)\hat{s}^2$$
$$-(1+14\hat{m}_s^2+\hat{m}_s^4)\hat{s}$$
$$+2(1+\hat{m}_s^2)(1-\hat{m}_s^2)^2], \tag{G4}$$

$$\alpha_4(\hat{s},\hat{m}_s,\hat{m}_l)=\left(1+\frac{2\hat{m}_l^2}{\hat{s}}\right)[(1-\hat{m}_s^2)^2-(1+\hat{m}_s^2)\hat{s}]. \tag{G5}$$

[1] CLEO Collaboration, M. S. Alam *et al.*, Phys. Rev. Lett. **74**, 2885 (1995).

[2] CLEO Collaboration, R. Balest *et al.*, in *Proceedings of the 27th International Conference on High Energy Physics*, Glasgow, Scotland, 1994, edited by P. P. Bussey and I. G. Knowles (IOP, London, 1995); CDF Collaboration, F. Abe *et al.*, Phys. Rev. Lett. **76**, 4675 (1996).

[3] J. Ellis and D. V. Nanopoulos, Phys. Lett. **110B**, 44 (1982); R. Barbieri and R. Gatto, *ibid.* **110B**, 211 (1982); T. Inami and C. S. Lim, Nucl. Phys. **B207**, 533 (1982); F. Gabbiani and A. Masiero, *ibid.* **B322**, 235 (1989).

[4] S. Bertolini, F. Borzumati, A. Masiero, and G. Ridolfi, Nucl. Phys. **B353**, 591 (1991).

[5] N. Oshimo, Nucl. Phys. **B404**, 20 (1993); J. Hewett, Phys. Rev. Lett. **70**, 1045 (1993); V. Barger, M. Berger, and R. J. N. Phillips, *ibid.* **70**, 1368 (1993); R. Barbieri and G. F. Giudice, Phys. Lett. B **309**, 86 (1993); J. L. Lopez, D. V. Nanopoulos, and G. T. Park, Phys. Rev. D **48**, 974 (1993); J. L. Lopez, D. V. Nanopoulos, G. T. Park, and A. Zichichi, *ibid.* **49**, 355 (1994); Y. Okada, Phys. Lett. B **315**, 119 (1993); R. Garisto and J. N. Ng, *ibid.* **315**, 372 (1993); M. A. Diaz, *ibid.* **322**, 207 (1994); F. M. Borzumati, Z. Phys. C **63**, 291 (1994); S. Bertolini and F. Vissani, *ibid.* **67**, 513 (1995); J. Wu, P. Nath, and R. Arnowitt, Phys. Rev. D **51**, 1371 (1995); P. Nath and R. Arnowitt, Phys. Lett. B **336**, 395 (1994); Phys. Rev. Lett. **74**, 4592 (1995); F. M. Borzumati, M. Drees, and M. M. Nojiri, Phys. Rev. D **51**, 341 (1995); J. L. Lopez, D. V. Nanopoulos, X. Wang, and A. Zichichi, *ibid.* **51**, 147 (1995); G. Kane, C. Kolda, L. Roszkowski, and D. Wells, *ibid.* **49**, 6173 (1994); M. Carena, M. Olechowski, S. Pokorski, and C. E. M. Wagner, Nucl. Phys. **B426**, 269 (1994); C. Kolda, L. Roszkowski, D. Wells, and G. Kane, Phys. Rev. D **50**, 3498 (1994).

[6] T. Goto and Y. Okada, Prog. Theor. Phys. **94**, 407 (1995).

[7] T. Goto, T. Nihei, and Y. Okada, Phys. Rev. D **53**, 5233 (1996).

[8] A. Ali, G. Giudice, and T. Mannel, Z. Phys. C **67**, 417 (1995).

[9] P. Cho, M. Misiak, and D. Wyler, Phys. Rev. D **54**, 3329 (1996).

[10] Y. Okada, M. Yamaguchi, and T. Yanagida, Prog. Theor. Phys. **85**, 1 (1991); Phys. Lett. B **262**, 54 (1991); J. Ellis, G. Ridolfi, and F. Zwirner, *ibid.* **257**, 83 (1991); H. E. Haber and R. Hempfling, Phys. Rev. Lett. **66**, 1815 (1991).

[11] K. Inoue, A. Kakuto, H. Komatsu, and S. Takeshita, Prog. Theor. Phys. **68**, 927 (1982); **71**, 413 (1984); L. Ibáñez and G. G. Ross, Phys. Lett. **110B**, 215 (1982); L. Alvarez-Gaumé, J. Polchinski, and M. B. Wise, Nucl. Phys. **B221**, 495 (1983); J. Ellis, J. S. Hagelin, D. V. Nanopoulos, and K. Tamvakis, Phys. Lett. **125B**, 275 (1983).

[12] A. Bouquet, J. Kaplan, and C. A. Savoy, Phys. Lett. **148B**, 69 (1984); Nucl. Phys. **B262**, 299 (1985); J. F. Donoghue, H. P. Nilles, and D. Wyler, Phys. Lett. **128B**, 55 (1983); L. E. Ibáñez and C. López, Nucl. Phys. **B233**, 511 (1984); L. E. Ibáñez, C. López, and C. Muñoz, *ibid.* **B256**, 218 (1985).

[13] B. Grinstein, M. J. Savage, and M. B. Wise, Nucl. Phys. **B319**, 271 (1989).

[14] M. Ciuchini *et al.*, Phys. Lett. B **316**, 127 (1993); Nucl. Phys. **B415**, 403 (1994); G. Cella *et al.*, Phys. Lett. B **325**, 227 (1994); A. Buras, M. E. Lautenbacher, M. Misiak, and M. Münz, Nucl. Phys. **B423**, 349 (1994).

[15] A. F. Falk, M. Luke, and M. J. Savage, Phys. Rev. D **49**, 3367 (1994); A. Ali, G. Hiller, L. T. Handoko, and T. Morozumi, this issue, Phys. Rev. D **55**, 4105 (1997).

[16] C. S. Lim, T. Morozumi, and A. I. Sanda, Phys. Lett. B **218**, 343 (1989).

[17] A. Ali, T. Mannel, and T. Morozumi, Phys. Lett. B **273**, 505 (1991).

[18] P. J. O'Donnel and H. K. K. Tung, Phys. Rev. D **43**, R2067 (1991); M. R. Ahmady, Ochanomizu University Report No. OCHA-PP-69, hep-ph/9511212 (unpublished); F. Krüger and L. M. Sehgal, Phys. Lett. B **380**, 199 (1996).

[19] E. Golowich and S. Pakvasa, Phys. Lett. B **205**, 393 (1988); Phys. Rev. D **51**, 1215 (1995); N. G. Deshpande, J. Trampetić, and K. Panose, *ibid.* **39**, 1461 (1989); J. M. Soares, *ibid.* **51**, 3518 (1995); **53**, 241 (1996).

[20] ALEPH Collaboration, D. Buskulic *et al.*, Phys. Lett. B **373**, 246 (1996); DELPHI Collaboration, P. Abreu *et al.*, *ibid.* **382**, 323 (1996); L3 Collaboration, M. Acciarri *et al.*, *ibid.* **377**, 289 (1996); OPAL Collaboration, G. Alexander *et al.*, *ibid.* **377**, 181 (1996).

[21] Particle Data Group, R. M. Barnett *et al.*, Phys. Rev. D **54**, 1 (1996).

[22] CDF Collaboration, F. Abe *et al.*, Phys. Rev. Lett. **75**, 613 (1995); **69**, 3439 (1992); D0 Collaboration, S. Abachi *et al.*, *ibid.* **75**, 618 (1995).

[23] L3 Collaboration, F. Abe *et al.*, Phys. Lett. B **350**, 109 (1995); ALEPH Collaboration, D. Decamp *et al.*, Phys. Rep. **216**, 253 (1992); DELPHI Collaboration, P. Abreu *et al.*, Phys. Lett. B **247**, 157 (1990); OPAL Collaboration, M. Z. Acrawy *et al.*, *ibid.* **248**, 211 (1990).

[24] J. P. Derendinger and C. A. Savoy, Nucl. Phys. **B237**, 307 (1984); see also J. A. Casas, A. Lleyda, and C. Muñoz, *ibid.* **B471**, 3 (1996); A. Kusenko, P. Langacker, and G. Segre, Phys. Rev. D **54**, 5824 (1996).